CHAPTER IV

RERULTS AND DISCUSSION

4.1 Stationary SEIRA Measurements: Self-Assembled Monolayers of ω-carboxylalkanethiols

It is well known that a SAM coated metal electrode is a useful tool in the biophysical field [61,62]. Proteins can be immobilized on SAMs and those monolayers mimic some features of biological interfaces, such as a hydrophobic core and charged surfaces. The local EF strength at the protein binding site can be controlled by varying the chain length of the monolayer [26]. Furthermore, SAMs are helpful to prevent denaturation upon protein adsorption on the metal electrode or during the spectro-electrochemical measurements.

In present work, monolayers of ω-carboxylalkanethiols are used to mimic the biomembrane for the protein, however the carboxyl end group can be also structurally modified (protonation/deprotonation) under the applied external EF. To investigate the stability of the monolayer, and to distinguish the monolayer spectra from those of the immobilized protein, potential-dependent investigations of the monolayer have been performed in stationary SEIRA measurements. They were done by varying the electrode potentials within the range which is of interest for the protein investigation.

4.1.1 Spectroscopic Characterization of the Structural Changes of Monolayers under the Electric Field Strength

The potential-dependent SEIRA difference spectra of ω-carboxylalkanethiol SAMs with various methylene units at the same applied electrode potential (+0.15 V) are shown in Figure 4.1. The reference spectrum was measured at -0.1 V. When the electrode potentials increased, a negative band between 1690-1700 cm^{-1}, which has been assigned to the C=O stretching mode of the carboxyl end group of the protonated monolayer, is observed together with two positive broad bands of the

deprotonated COO^- headgroup, the anti-symmetric (between 1555-1569 cm^{-1}) and the symmetric (between 1380-1409 cm^{-1}) stretching vibration [63-66]. This shows that the monolayer end group deprotonates as expected with raising electrode potentials above -0.08 V. At potentials below the reference potential, protonation is observed by the inverse spectral effects (Figure 4.2). The band between 1406-1435 cm^{-1} has been assigned to a combination of the symmetric COO^- stretching vibration and the CH_2 scissor bending vibration [65]. Nevertheless, at frequencies around and below 1470/1430 cm^{-1}, spectral contributions of the Si-O stretching modes of the prism may occur due to the related reduced transmission of the prism at the lower frequencies and slight temperature fluctuations (spectrum of air in Figure 4.1). Therefore, the S/N is even worse at the frequency range below 1250 cm^{-1}.

As one can see in Figure 4.1, the spectral pattern of the protonated and deprotonated monolayer is consistent also for all SAM chain lengths. Only slight peak shifts and differences in peak intensity are observed under the same condition (pH, monolayer concentration and ionic strength). The difference in peak intensities of the protonated and deprotonated species for different SAM-lengths depends on the surface properties, i.e. pK_a, of the SAM. The band intensity changes of the protonated and deprotonated species decrease with increasing alkyl chain lengths because the proton affinity of the carboxyl tail-group is stronger for the short monolayer due to changes in their surface pKa values (from 5 to 8 for C1-SAM relative to C15-SAM) [38]. The band position of the protonated species is shifted to higher frequencies (shift from ca. 1700 to ca. 1730-1740 cm^{-1}) with increasing methylene unit due to a weaker hydrogen-bonding interaction [64], while hardly any deprotonation can be observed for the alkyl chain length longer than C5-SAM.

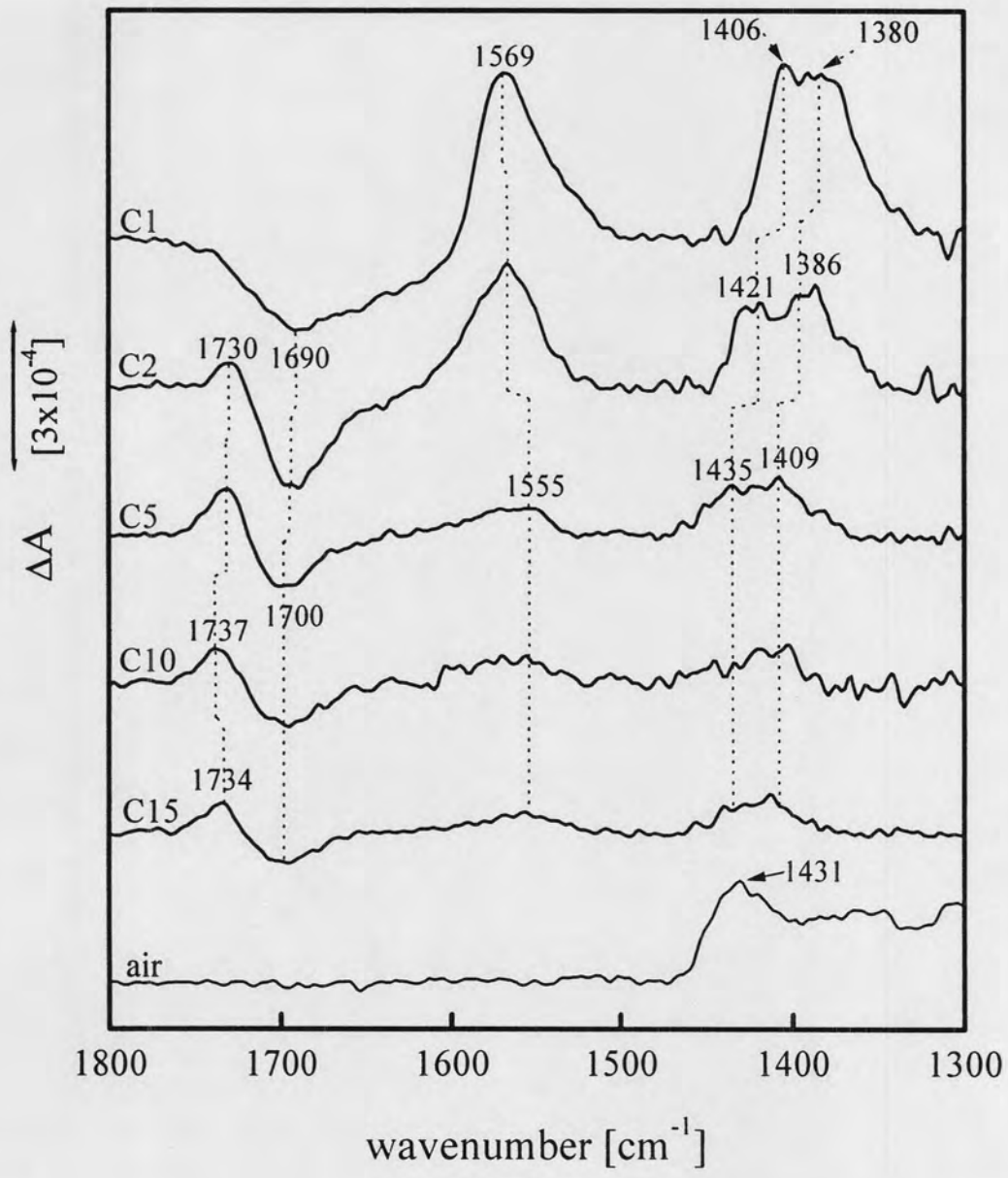

Figure 4.1 The potential-dependent SEIRA difference spectra of C1-, C2-, C5-, C10- and C15-SAMs. The spectra were taken at an electrode potential of +0.15 V (the reference spectrum was measured at -0.1 V). The experiments were carried out at the ionic strength of 22 mM (pH 7.0). The time/temperature dependent effects in an ATR FT-IR spectrum of air were measured with a Si-prism.

4.1.2 The Potential Range of Reversible Changes in the SEIRA Difference Spectra of ω-carboxylalkanethiol Self-Assembled Monolayers

The potential-dependent SEIRA difference spectra of the monolayers were acquired in a range between -0.2 to +0.2 V, as shown exemplarily in Figure 4.2. This covers the potential range, in which the investigation of orientational and structural changes of peptide segments of Cyt-c has been carried out. The spectra were measured by varying the potentials from -0.2 to +0.2 V. After a potential change, the potential was always set back to the reference value at -0.1 V. The reversibility of changes in the monolayer spectra has been investigated at the reference value of -0.10 V by probing the change between spectrum before and after the potential jumps.

An example of the reversibility of changes in monolayer spectra measured at -0.10 V is shown in Figure 4.3. The difference is very small, absorbance change is ca. $4x10^{-5}$, only a broad band at 1650 cm^{-1} can be observed, which is assigned to the OH bending mode vibration of absorbed H_2O molecules. There might be also some overlap with the corresponding band of some ice adsorptions on the detector window for this particular measurement. Ice adsorption is the origin of the sharp absorption band in the high-frequency range at 3250 cm^{-1}, which is assigned to the OH stretching vibration of H_2O molecules. The observed changes appear to be almost constant after jumps to more positive potentials. The same pattern of reversible changes is observed for the other monolayer chain lengths as shown in Figure 4.4, except for C1-SAM, where some irreversibility in spectral changes can be attributed to reorientation effects (vide infra). Slight variations in the frequency range around and below 1430 cm^{-1}, as mentioned above, might be attributed to spectral artifacts from the Si-oxide absorptions and are caused by small temperature fluctuations (spectrum of C2 in Figure 4.4).

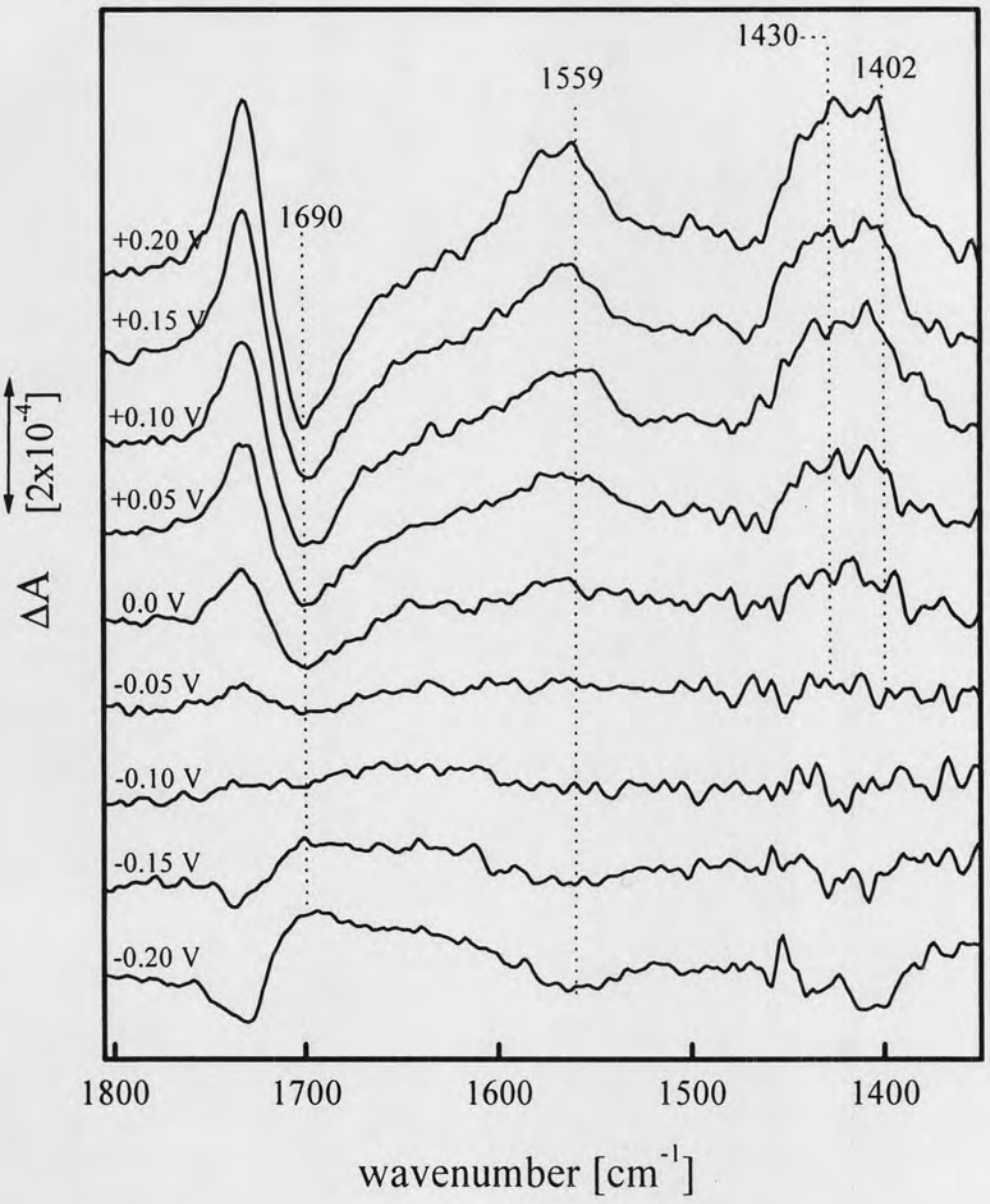

Figure 4.2 Example of series of the potential-dependent SEIRA difference spectra of C5-SAM measured at -0.20, -0.15, -0.10, -0.05, 0.00, 0.05, 0.10, 0.15, and 0.20 V, respectively. The reference spectrum was collected at -0.10 V. The experiments were carried out at the ionic strength of 22 mM (pH 7.0). Each spectrum was measured after waiting at the certain potential for 60 s (3 min/spectrum).

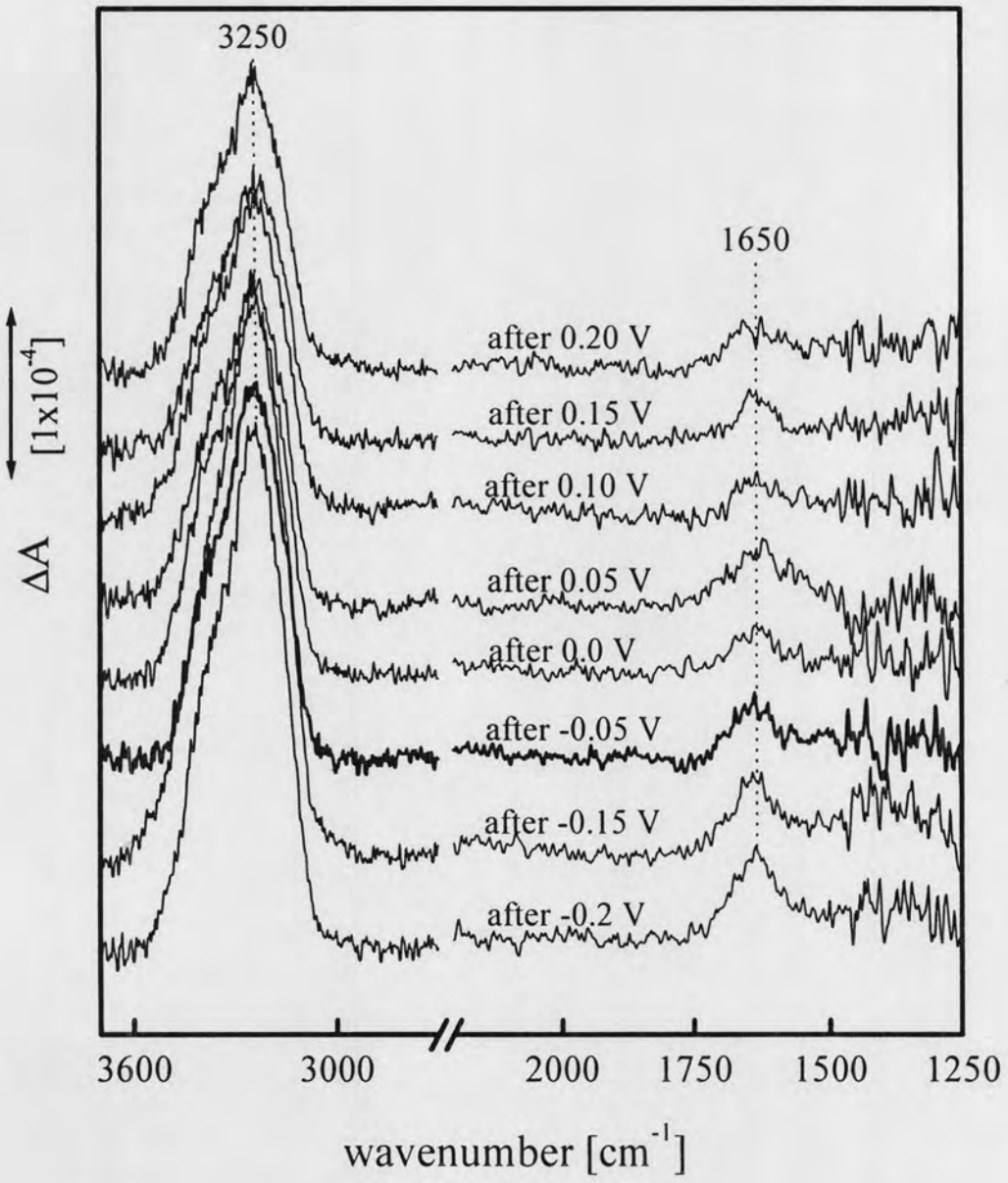

Figure 4.3 The series of reversible spectral changes of C5-SAM at the reference potential of -0.10 V after the potential jumps to -0.20, -0.15, -0.05, 0.00, 0.05, 0.10, 0.15, and 0.20 V, respectively; recalculated relative to the reference spectrum before the respective potential jump.

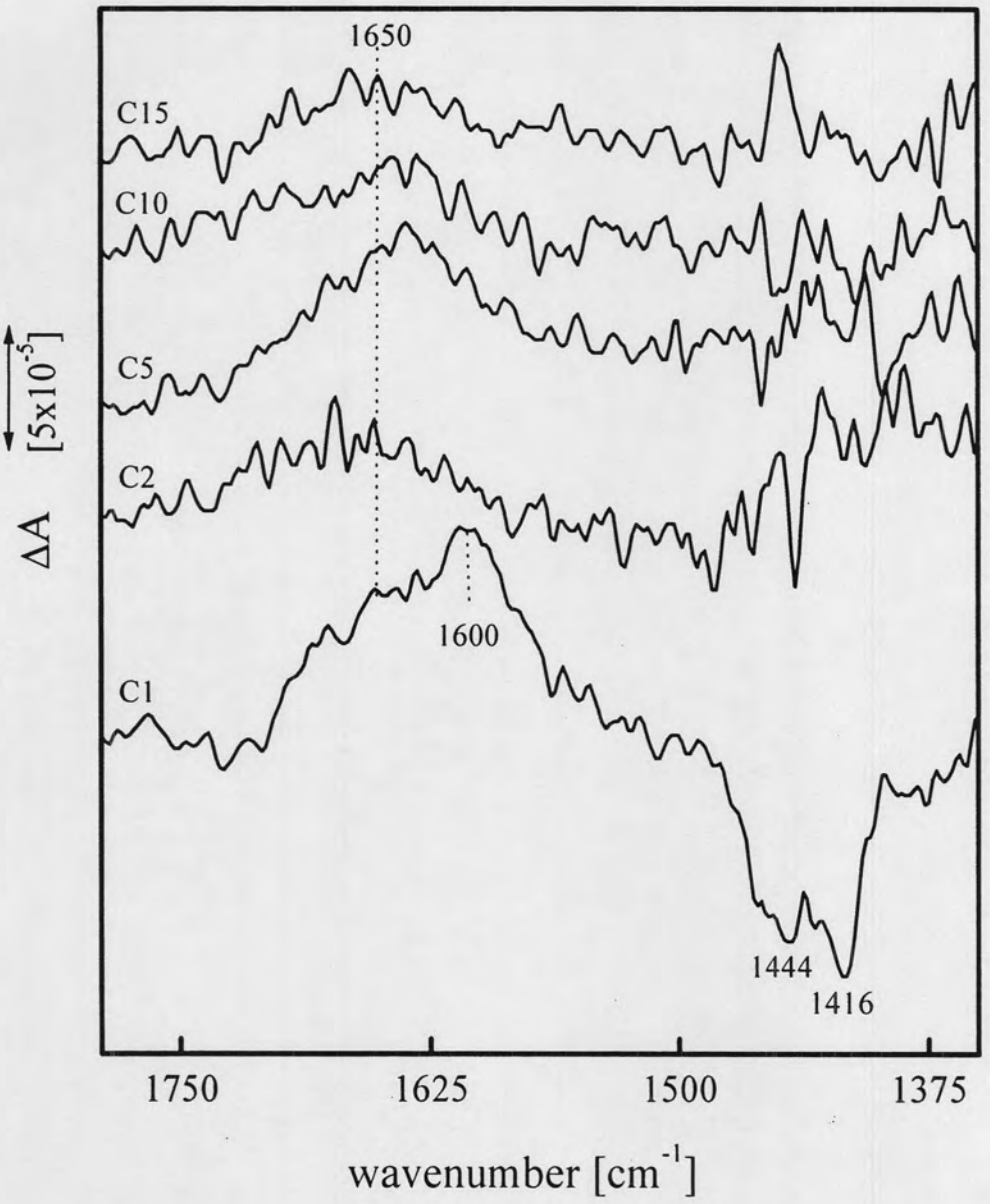

Figure 4.4 The reversible spectral changes of monolayers at the reference potential of -0.10 V for C1-, C2-, C5-, C10- and C15-SAMs; recalculated relative to the reference spectrum before the respective potential jump.

For C1-SAM, which is less stable due to the weaker hydrophobic interaction of the short alkyl chain, some minor irreversible changes at the reference potential (-0.1 V), as shown in Figure 4.5, might be caused by a reorientation. Furthermore, a reductive desorption of the monolayer and an adsorption of water molecules takes place at the same time. It is more pronounced after jumped to negative potentials (<-0.15 V). Indicative for the reorientation of monolayer is a positive band of the asymmetric COO^- stretching at ca. 1600 cm^{-1} with the corresponding two negative bands of the symmetric COO^- stretching vibrations are observed at 1444 and 1416 cm^{-1}, Figure 4.5a and b. More details will be discussed in Section 4.1.3. The band at 1444 cm^{-1} is a combination band with the CH_2 scissoring vibration. After potential jumps to negative potential at -0.15 and -0.2 V, the reductive desorption of the monolayer is characterized by two negative bands at 1444/1416 cm^{-1} and a broad negative band underneath at ca. 1545 cm^{-1}, which is found at the same time together with the adsorption of water molecules at ca. 1650 cm^{-1}. After potential jumps to more positive values, however, the band of water absorption is less pronounced, and only reductive desorption of monolayer is found at the reference value of -0.1 V. However, the observed spectral changes are still very small compared to those in the corresponding difference spectra at positive potentials (Figure 4.6). The potential-dependent SEIRA difference spectra of C1-SAM, as shown in Figure 4.6 typically exhibit the protonated and deprotonated forms of the reactive carboxyl end-group, while the reorientation is not found at potentials larger than the reference potential. At more negative potential (< -0.15 V), reorientation as well as a reductive desorption of the monolayer and water absorption occur at the same time.

In summary, the reversibility of changes in the monolayer spectra was investigated at the reference potential (-0.1 V) and in the difference spectra as function of electrode potential. In the potential range between -0.1 and +0.2 V, the latter investigations reveal only a potential-dependent protonation/deprotonation and some minor water adsorption is found as function of time at the reference potential. Some irreversible changes of short monolayers (C1-SAM) at negative potentials (<-0.15 V) are caused by reorientation, reductive desorption of the SAM and water absorption which takes place at the same time. However, such irreversible changes of monolayer spectra have not been seen in a potential range between -0.2 and +0.2 V for the other SAM chain

lengths (C2-, C5-, C10- and C15-SAM). Therefore, the observed spectral changes are reversible in the potential range of interest for investigating Cyt-c bound to these monolayers. However, a new reference spectrum has to be acquired to compensate the H_2O absorption, especially for the shortest monolayer (C1-SAM) where additionally reorientation/irreversible effects occur as function of time. Furthermore, reversible spectral changes are observed in a larger potential range (between -0.60 and +0.40 V) for long SAM lengths (C10-SAM).

Irreversible changes of potential-dependent difference spectra of monolayer are observed when potential jumps were carried out to very negative potential. The difference spectrum of C10-SAM, at -0.7 V, reveals a strong adsorption of water molecules which is seen by the positive band at 1627 cm^{-1} (Figure 4.7). This band has the same intensity changes compared to the band of the protonated monolayer at 1692 cm^{-1}. The observable spectral changes at the reference value (+0.1 V) after jumps to negative potentials of -0.7 V are very large relative to the reference spectrum before the potential jump (Figure 4.8). After jumps to -0.7 V, the spectrum is preserved and does not change from the spectrum at -0.7 V. C2-SAM also reveals irreversible changes in the potential-dependent SEIRA difference spectra. As one can see at a potential of -0.4 V (Figure 4.9), a reductive desorption of the monolayer take place which can be seen on hands of the negative bands of the asymmetric COO^- stretching (ca. 1578 cm^{-1}) and the two modes involving the symmetric COO^- stretching (1400 and 1430 cm^{-1}). At the same time, adsorption of H_2O molecules takes place which is seen by the broad positive band at 1650 cm^{-1}. After jumped to negative potentials of -0.4 V, the spectral feature is conserved and does not change when the potential is switched back to -0.1 V. Moreover, as already observed for the C1 monolayer some reorganization takes place as function of time (vide infra), which is characterized by a positive band of the asymmetric COO^- vibration at 1578 cm^{-1} with corresponding negative peaks of the symmetric COO^- vibrations at 1430 and 1400 cm^{-1}. Thus, one reason for irreversible changes might be related to potential jumps to very negative potentials where a reductive desorption occurs. However, an imperfect packing of the SAM, especially for short monolayers on the Au-electrode could be also a reason of irreversible changes, such as a reorientation as function of time.

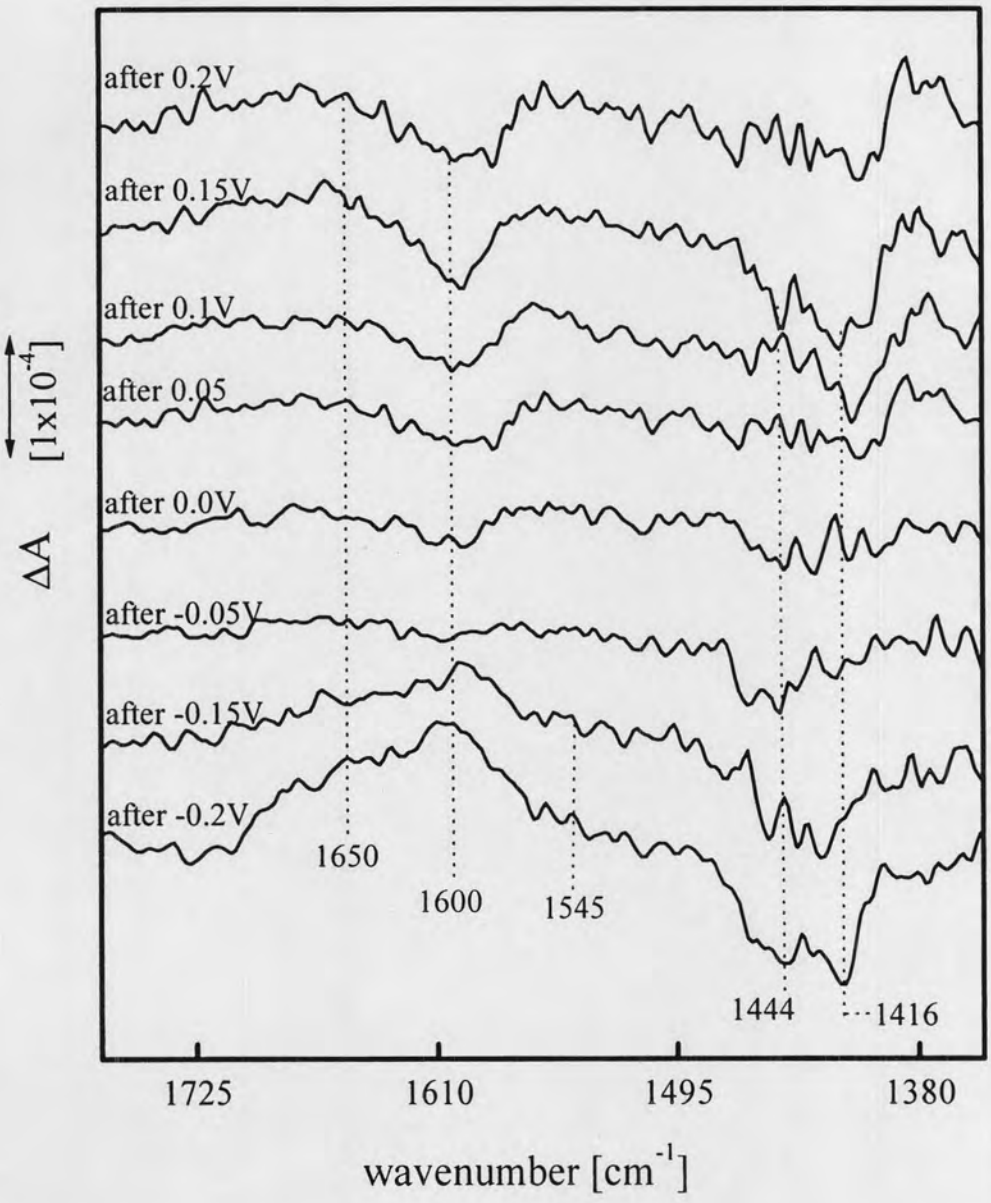

Figure 4.5 The series of irreversible spectral changes of C1-SAM at the reference potential of -0.10 V after potential jumps to (a) -0.20 V, (b) -0.15 V, (c) -0.05 V, (d) 0.00 V, (e) +0.05 V, (f) +0.10 V, (g) +0.15 V and (h) +0.20 V, respectively; recalculated relative to the reference spectrum before the potential jump.

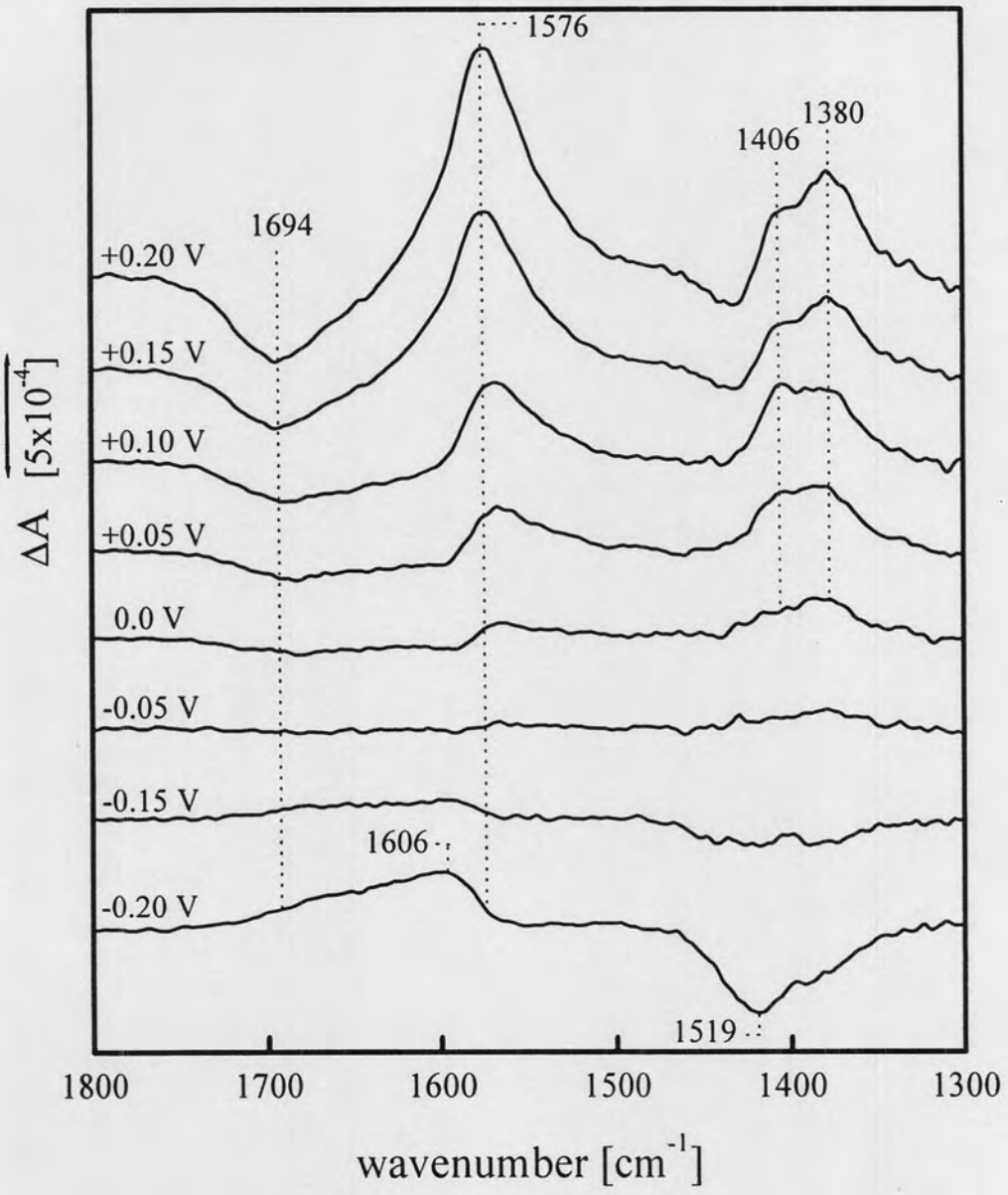

Figure 4.6 Series of the potential-dependent SEIRA difference spectra of C1-SAM measured at -0.20, -0.15, -0.05, 0.00, 0.05, 0.10, 0.15 and 0.20 V, respectively. The reference spectrum was collected at -0.10 V. The experiments were carried out at the ionic strength of 22 mM (pH 7.0). Each spectrum was measured after waiting at a certain potential for 60s (3 min/spectrum).

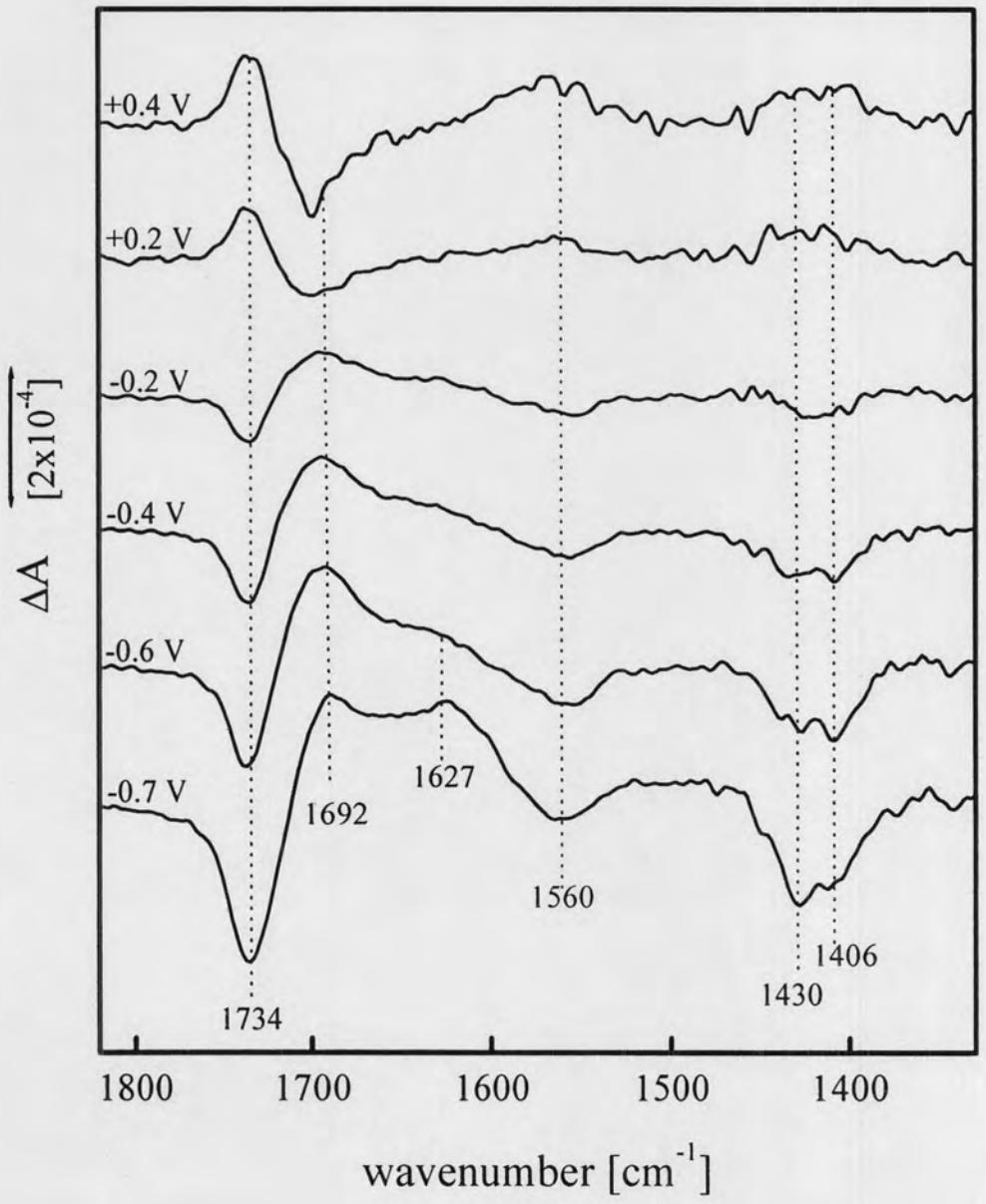

Figure 4.7 The potential-dependent SEIRA difference spectra of C10-SAM measured at +0.4, +0.2, -0.2, -0.4, -0.6 and -0.7 V, respectively. The reference spectrum was collected at +0.1 V. The experiments were carried out at the ionic strength of 22 mM (pH 7.0). Each spectrum was measured after waiting at a certain potential for 60 s (3 min/spectrum).

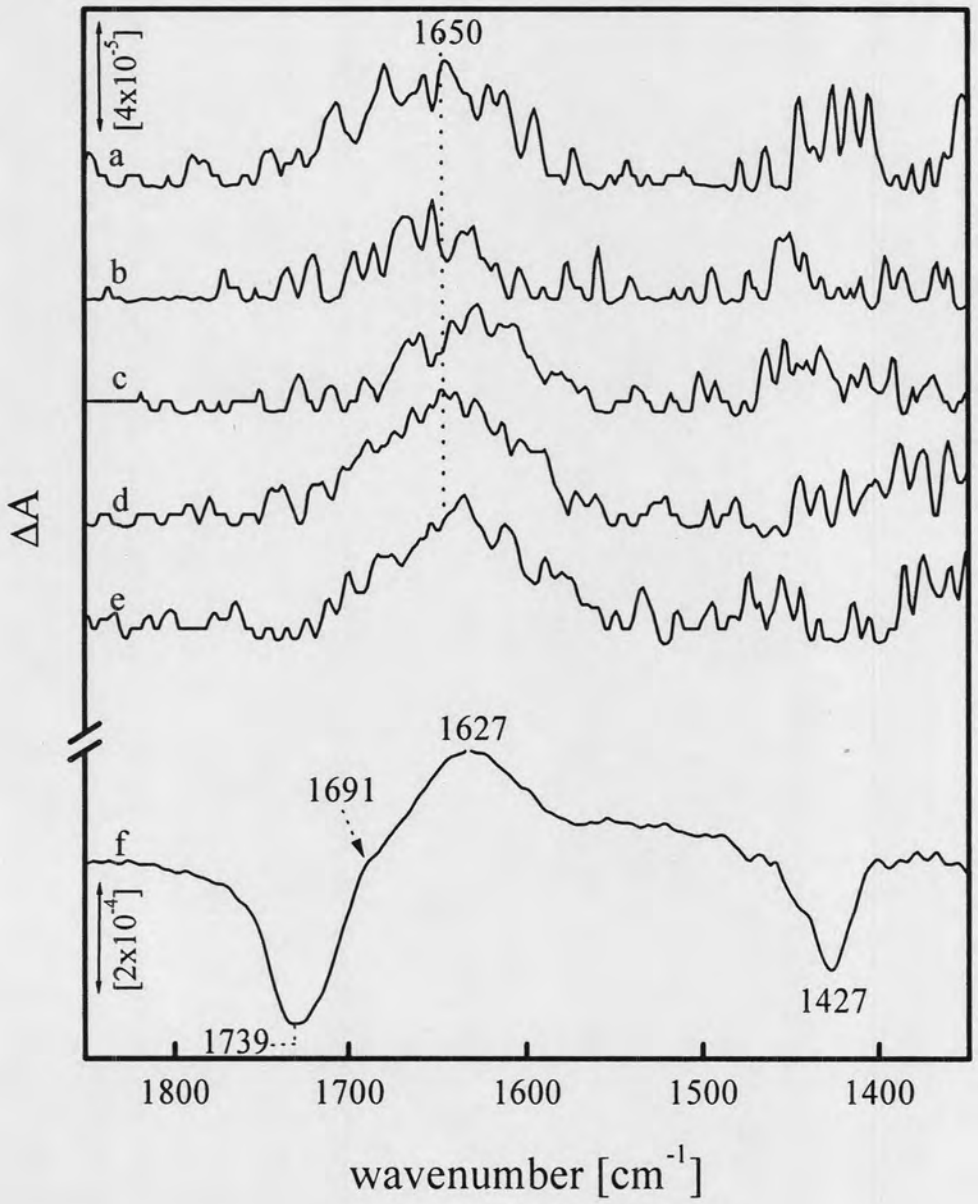

Figure 4.8 The series of irreversible spectral changes of C10-SAM at the reference potential of +0.10 V after potential jumped to (a) +0.4 V, (b) +0.2, (c) -0.2, (d) -0.4, (e) -0.6 and (f) -0.7 V, respectively; recalculated relative to the reference spectrum before the potential jump. The experiments were carried out at an ionic strength of 22 mM (pH 7.0). Each spectrum was measured after waiting at a certain potential for 60s (3 min/spectrum).

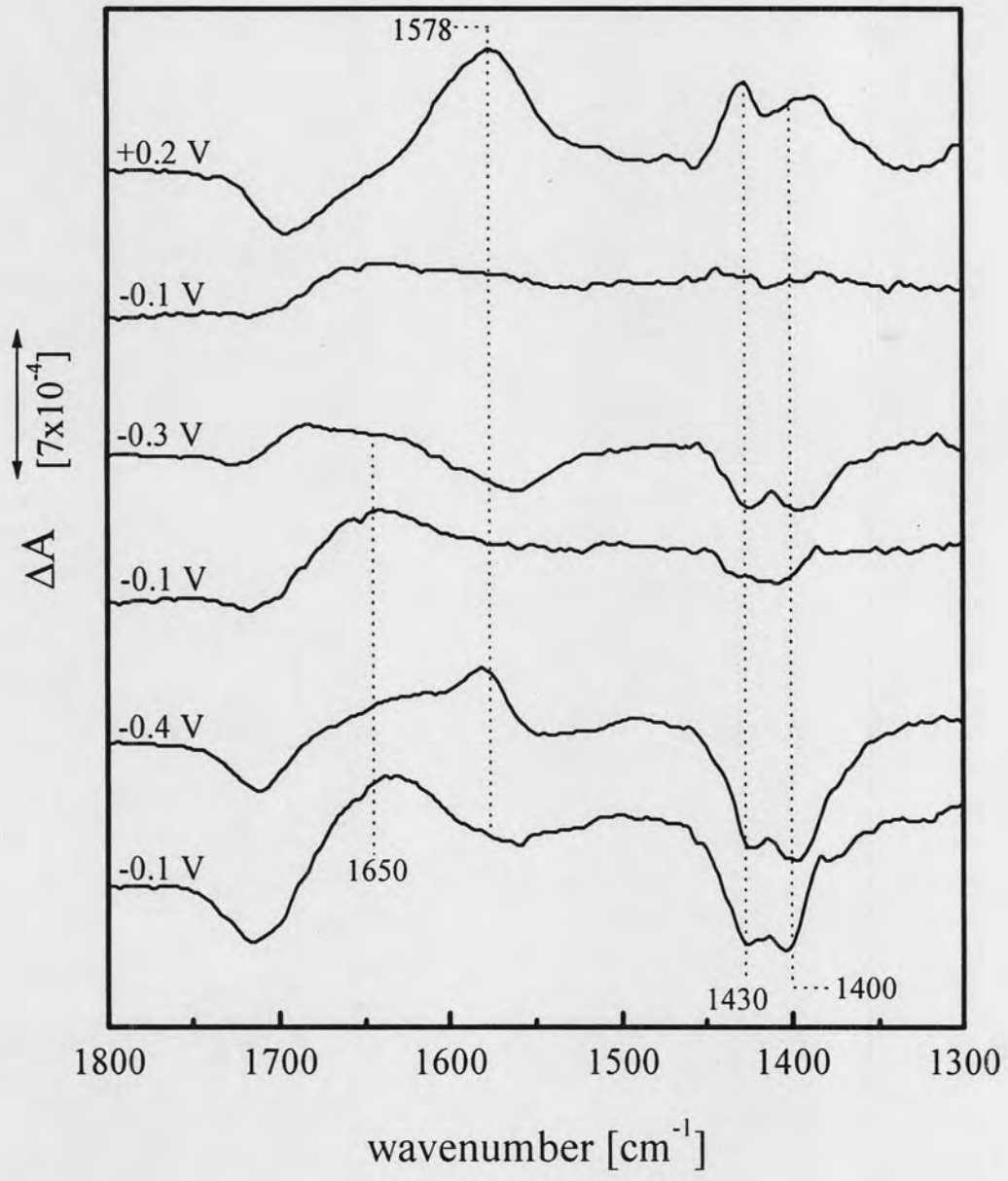

Figure 4.9 The irreversible changes of the potential-dependent SEIRA difference spectra of C2-SAM after jumps to very negative potentials measured at +0.20, -0.30 and -0.40 V, respectively. The reference spectrum was taken at -0.10 V. The experiments were carried out at the ionic strength of 22 mM (pH 7.0). The irreversible changes in the monolayer spectra measured at -0.10 V are obvious after recalculating it relative to the reference spectrum before the potential jump. The spectra series at varied electrode potentials is displayed here (from the top to the bottom).

4.1.3 Stability and Reorientation of Short Monolayers (C1-SAM)

Due to a less ordered SAM formation on the Au-electrode surface, more reorientation is found for short monolayers than for the longer SAM length, especially in the case of the C1-SAM, which has only one methylene group in the alkyl chain. Two structures of the C1-SAM were found to be formed on the Au-surface when an assembling time of monolayer on the Au-surface is short (only 2 hs), as reflected by a negative band of the protonated species at 1695 cm^{-1} is found together with a positive band of the COO^- anti-symmetric (1580 cm^{-1}) and a negative band of the COO^- symmetric (1390 cm^{-1}) stretching vibration, Figure 4.10.

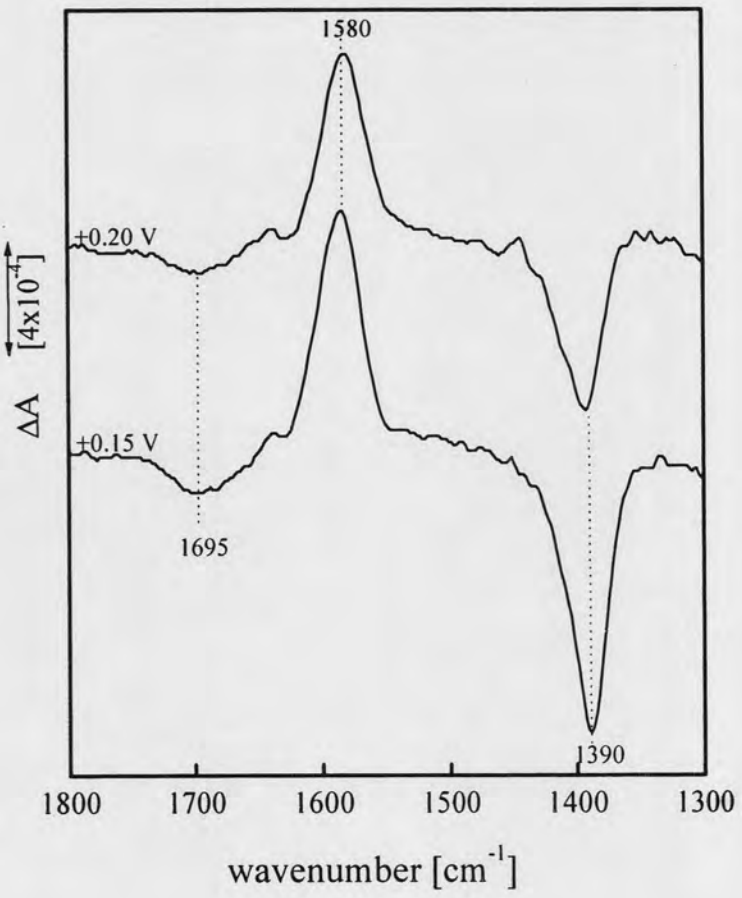

Figure 4.10 The potential-dependent SEIRA difference spectra of C1-SAM at +0.15 and +0.20 V, respectively. The reference spectrum was collected at -0.10 V. The experiments were carried out at the ionic strength of 22 mM (pH 7.0).

While the first two spectral changes are caused by a simple protonation/deprotonation, the negative band at 1390 cm^{-1} is due to the reorientation of the monolayer from the less stable structure, which is formed via both thiolate and carboxylate binding to the metal-surface (Figure 4.11a), to the more stable form (Figure 4.11b). Such a self-assembly process of the monolayer has been proposed for a Ag-electrode, but it is likely to hold also for a Au-surface [39]. For the structure in Figure 4.11a, only the symmetric COO^- stretching band is detectable, because the C=O of the protonated COOH and the anti-symmetric COO^- vibrations are not SEIRA active since the corresponding dipole moment changes are parallel to the surface. It is, therefore, concluded that the C1-SAM is reoriented as function of time (independent from a potential jump) to a more stable form in which only the thiolate group is adsorbed to the metal surface (Figure 4.11b), reflected by a decrease of a negative peak at 1390 cm^{-1}. To avoid the undesired restructuring during the SEIRA measurements, the metal surface should be exposed to the monolayer solution about 12 hs for a good coverage and the monolayer solution should be prepared freshly every time.

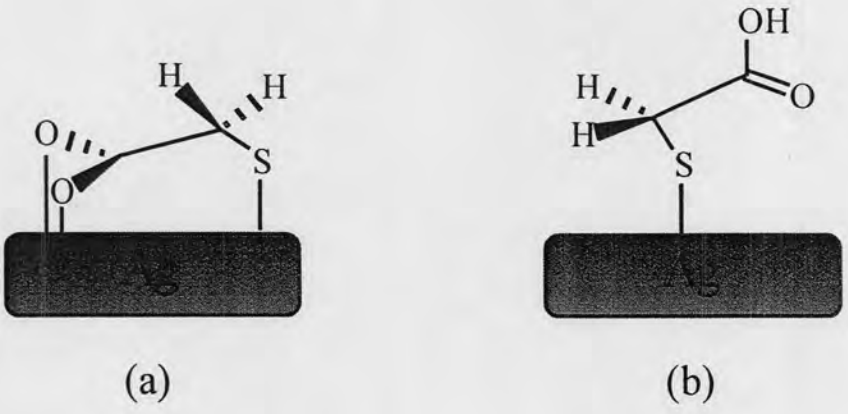

Figure 4.11 A schematic diagram of the monolayer of mercaptoacetic acid adsorbed (a) with carboxylate and thiolate group and (b) only with the thiol group; e.g. on a Ag surface [39].

4.1.4 Spectral Contributions of Monolayers

Despite the similarities of the SEIRA difference spectra of immobilized Cyt-c on carboxyl-terminated SAM at various chain lengths (more detail will be discussed in next section), there are also differences between the spectra reflected by the effect of the local EF strength. Figure 4.12 shows the overlay of the difference spectra of Cyt-c adsorbed on a short (C1-SAM) and on a long (C15-SAM) monolayer, and the corresponding pure monolayer difference spectrum measured at the same potential of +0.1 V using the spectrum of -0.1 V as reference. The SEIRA difference spectra of Cyt-c reveal several bands clearly distinguishable from the broad bands of the monolayers, e.g., the intensive sharp band at 1693 cm^{-1} of the adsorbed Cyt-c is clearly distinguished from the broad band at 1691 cm^{-1} (protonated COOH) belonging to the C1-SAM and C15-SAM. The other important Amide I difference bands at 1673 and 1660 cm^{-1} are also entirely isolated from the monolayer spectra as they reveal the much more intense peak height. However, the broad overlapping bands between ca. 1400-1560 cm^{-1} are more difficult to analyse, related to the effect of potential-dependent protonation/deprotonation of the SAM end groups. In this region, the antisymmetric and symmetric COO^- vibrational modes interfere with the Amide II and Amide III bands, respectively. This interference is particularly severe for the short monolayers, i.e., C1-SAM, due to the relatively low pK_a value (ca. 6). The effect is much less pronounced when Cyt-c was adsorbed to the SAM with long alkyl lengths, i.e., C10- and C15-SAM, which are less acidic.

Figure 4.13 shows the peak intensities of the adsorbed Cyt-c on C1- and C15-SAM, and those derived from the corresponding pure C1- and C15-SAM difference spectra. The peak height of the 1693-cm^{-1} band of Cyt-c adsorbed on C1-SAM and C15-SAM is much more intense than the corresponding bands of the pure monolayer. For the Amide II and Amide III bands in the difference spectra, however, an overlap with the spectral contributions of the SAMs is critical, especially for the C1-SAM. Considering the C15-SAM, the peak intensities of the monolayer spectra are almost negligible and thus hardly overlap with the spectra of the adsorbed Cyt-c. However, due to the reorientation and interaction changes of the monolayer tailgroups, simple

subtraction of the spectral monolayer from the spectra of immobilized Cyt-c is also critical, especially for C1-SAM.

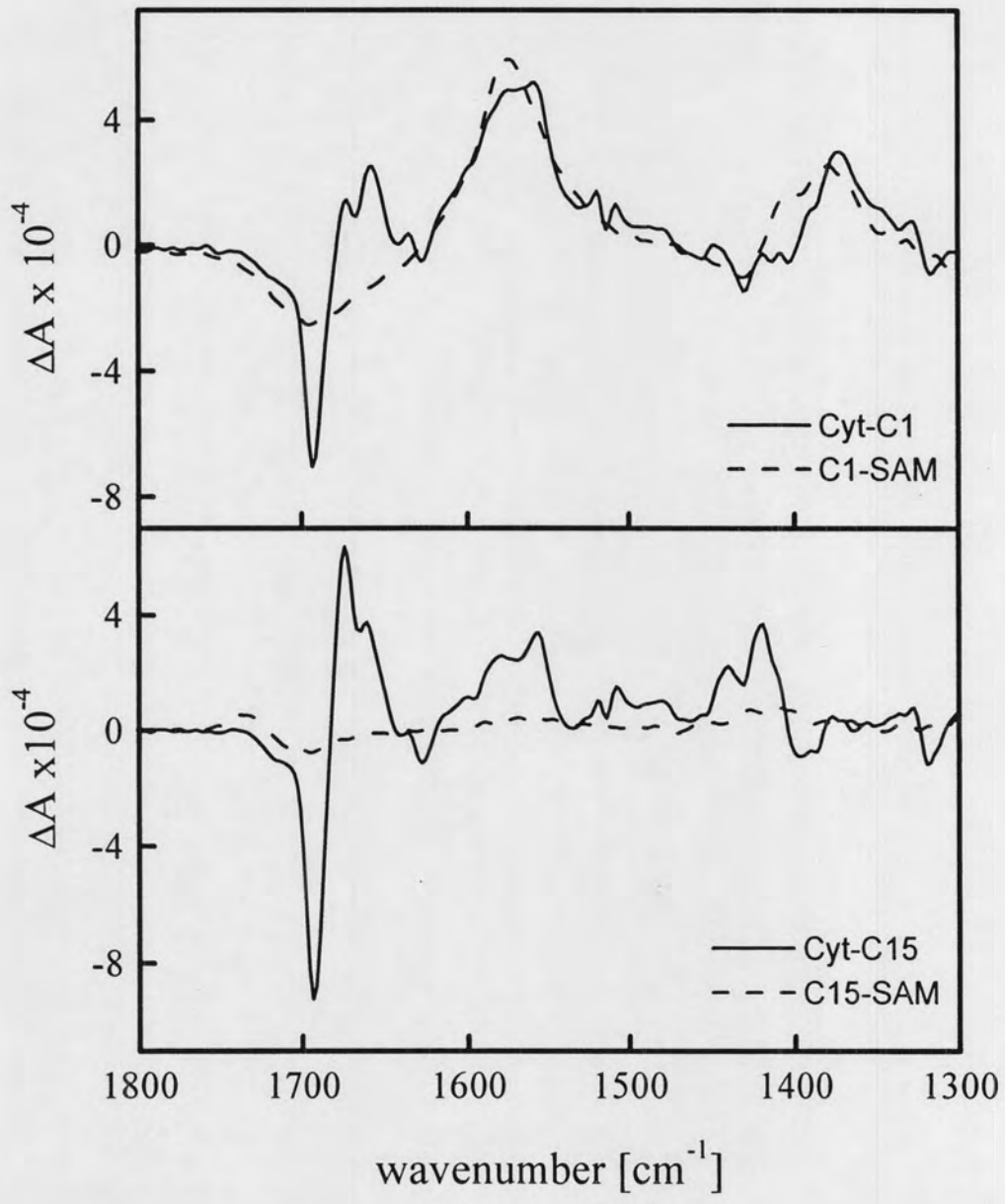

Figure 4.12 The potential-dependent SEIRA difference spectra (Cyt-c fully oxidized at +0.10 V minus fully reduced at -0.10 V); the overlay of the C1-SAM (top) and C15-SAM (bottom) difference spectra with and without the presence of Cyt-c.

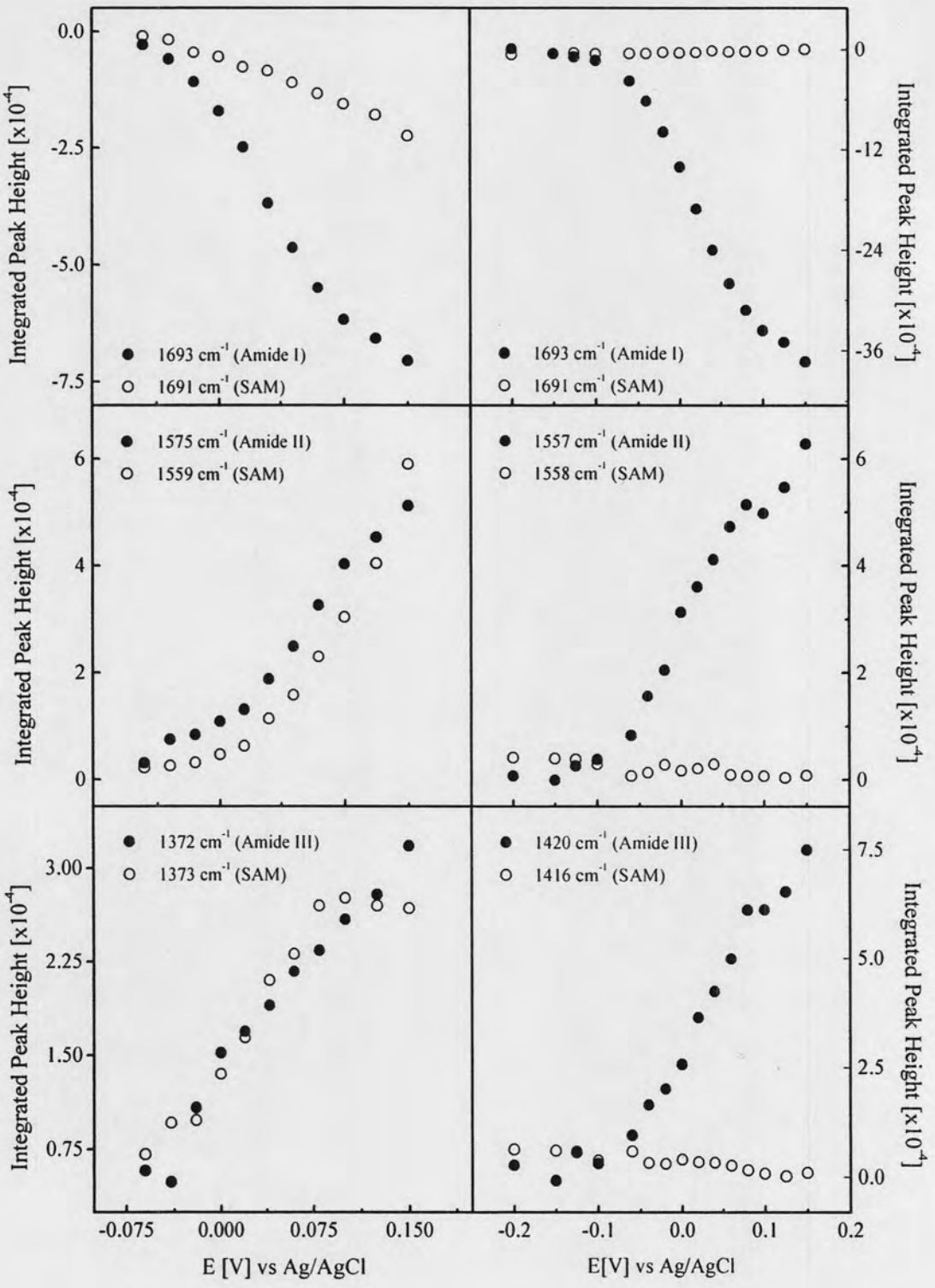

Figure 4.13 The plot of peak intensities as function of the electrode potential of the corresponding pure monolayer spectra (circle, open) and additionally adsorbed Cyt-c (circle, solids) on C1-SAM (left) and C15-SAM (right).

4.2 Stationary SEIRA Investigations: Cytochrome c

4.2.1 Characterization of Cytochrome c

Cyt-c electrostatically immobilized on ω-carboxylalkanethiol coated Au electrodes exhibits the same SEIRA absorption spectra for all SAM lengths, which are almost identical to the IR spectrum of native Cyt-c in solution. Minor deviations can be identified upon adsorption, e.g. a more pronounce negative band at 1700 cm^{-1} can be revealed. This is caused by a desorption of SAM-molecules accompanied by an absorption of water molecules on the Au electrode, which is always the obstacle for the IR technique investigating protein. Due to pronounced band overlaps in the absorbance spectra, their second (2^{nd})-derivatives are derived to determine the frequencies in a more reliable manner. A comparison of the 2^{nd}-derivative spectra of immobilized Cyt-c with that of Cyt-c in the bulk-solution is nearly identical with respect to the observed frequencies, only slight differences in the relative band intensities are found, Figure 4.14. Two major bands of the Amide I and Amide II maxima are located at 1659 and 1551 cm^{-1}, respectively, which are representative for an α-helix structure [67,69]. The band at the "higher edge" of the Amide I region at 1680 cm^{-1} is assigned to a turn structure and those at lower frequencies of 1633-cm^{-1} band as well as the small band at 1614 cm^{-1} originates from a β-sheet structure [32,67-69]. A stretching mode of the heme moiety at 1597 cm^{-1}, which is also present in the resonance Raman spectrum, is found as well as the phenyl ring vibration of a tyrosine residue at 1517 cm^{-1} [6,32]. The peak assignment of these bands has been guided by the X-ray crystallographic and NMR structure data [25,70-73]. A more detailed assignment of the redox-linked structural changes will be discussed in the context of the SEIRA difference spectroscopy results (vide infra).

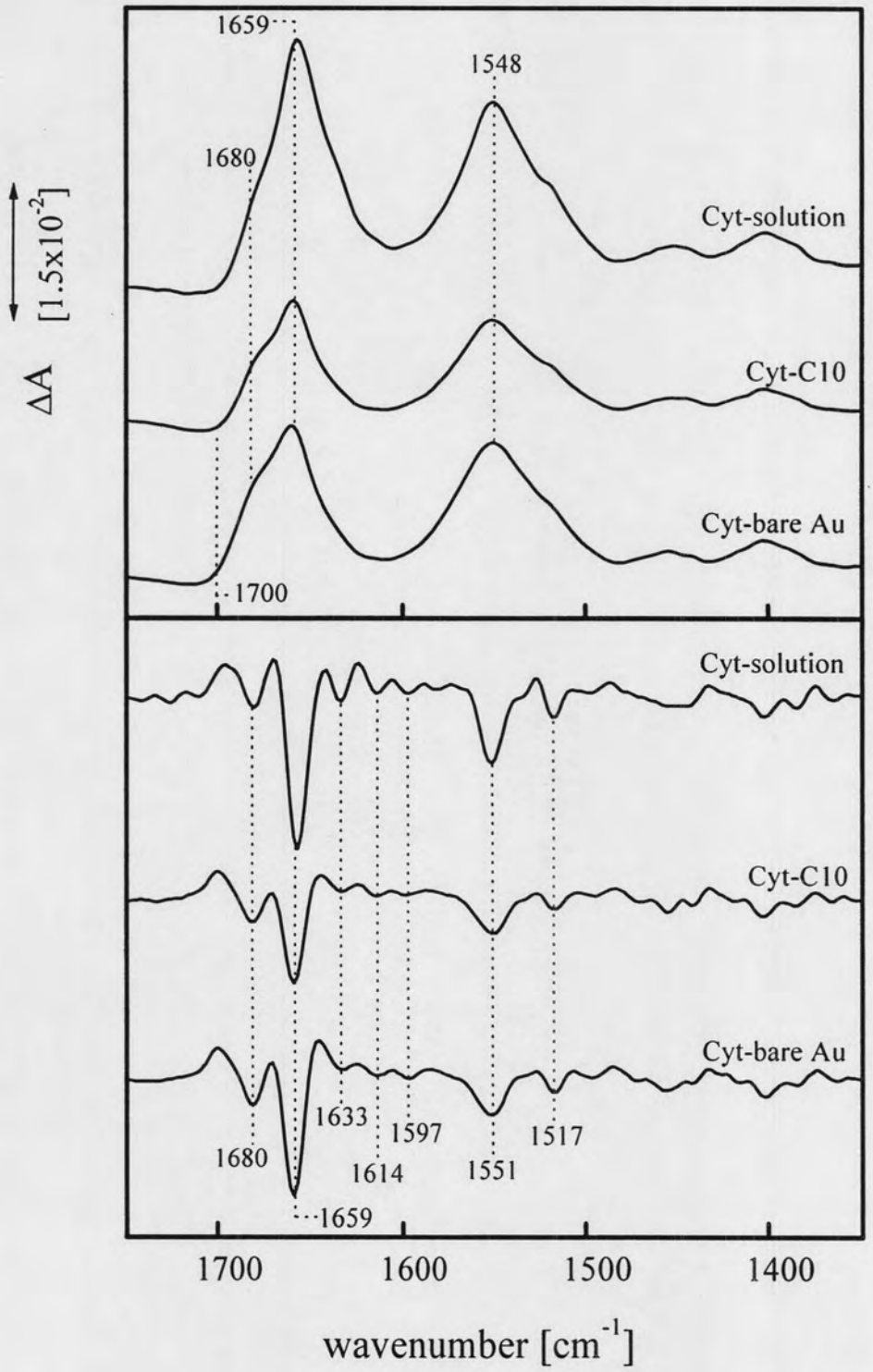

Figure 4.14 The absorbance spectra (top) and their second (2^{nd})-derivatives (bottom) of Cyt-c in a bulk-solution, and immobilized on C10-SAM and bare Au-electrode. All spectra were measured at the open circuit potential (OCP), which is always >0 V.

4.2.2 Redox-Linked Structural Changes of Immobilised Cytochrome c

SEIRA spectroscopy is operated in the difference mode to enhance the sensitivity of the technique. To probe potential-dependent spectral changes, difference spectra were constructed from SEIRA spectra measured at various electrode potentials using the SEIRA spectrum measured at -0.1 V as the reference. At this negative potential, the immobilised Cyt-c is in the fully reduced state such that SEIRA difference spectra obtained from the measurements at more positive potentials reflect the redox-linked structural and orientational changes of the SAM/Cyt-c complex, which have also been observed in a previous SEIRA study by Ataka and Heberle [6]. Figure 4.15 and 4.16 display such SEIRA difference spectra of immobilized Cyt-c on C15-SAM and on C10-SAM at different buffer concentrations corresponding to different ionic strengths. The most prominent difference signals are observed in the region of the Amide I (1620 – 1700 cm^{-1}) and Amide II modes (1540 – 1570 cm^{-1}) of the polypeptide backbone. Assignments for the Cyt-c difference (IR) spectra of Amide I modes have been discussed by many authors [6,32,74,75]. Accordingly, the negative band at 1693 cm^{-1} has been assigned to a β-turn type III segments 14-19 or 67-70 of the reduced Cyt-c whereas its counterpart in the oxidised form is attributed to the 1673-cm^{-1} band. Correspondingly, the 1666- and 1660-cm^{-1} bands were tentatively attributed to the Amide I bands of a β-turn type II of reduced and oxidised Cyt-c, respectively, although the assignment to specific peptide segments is less clear and the assignment to an α-helix segment cannot be ruled out [6,68,74].

The comparison of the difference spectra measured at various ionic strength of 22 mM and 66 mM display changes in the relative band intensities particularly for Cyt-c immobilised on C15-SAM while the band positions remain unchanged. Taking the positive signals at ca. 1442 and 1420 cm^{-1} assigned by Susi and Byler [76] to CH_2 and CH_3 bending modes as a reference, the intensity of the 1693-cm^{-1} band decreases at higher ionic strength whereas the 1660-cm^{-1} band and, to a smaller extent, also the 1673-cm^{-1} band gain intensity. At an ionic strength of 22 mM, the 1660-cm^{-1} band exhibits a higher intensity on C10-SAM as compared to C15-SAM, and it further increases with raising the ionic strength to 66 mM. At this ionic strength the intensity

pattern of the 1673- and 1660-cm^{-1} bands is the same on C15-SAM where, however, a distinctly weaker signal at 1693 cm^{-1} is observed compared to C10-SAM.

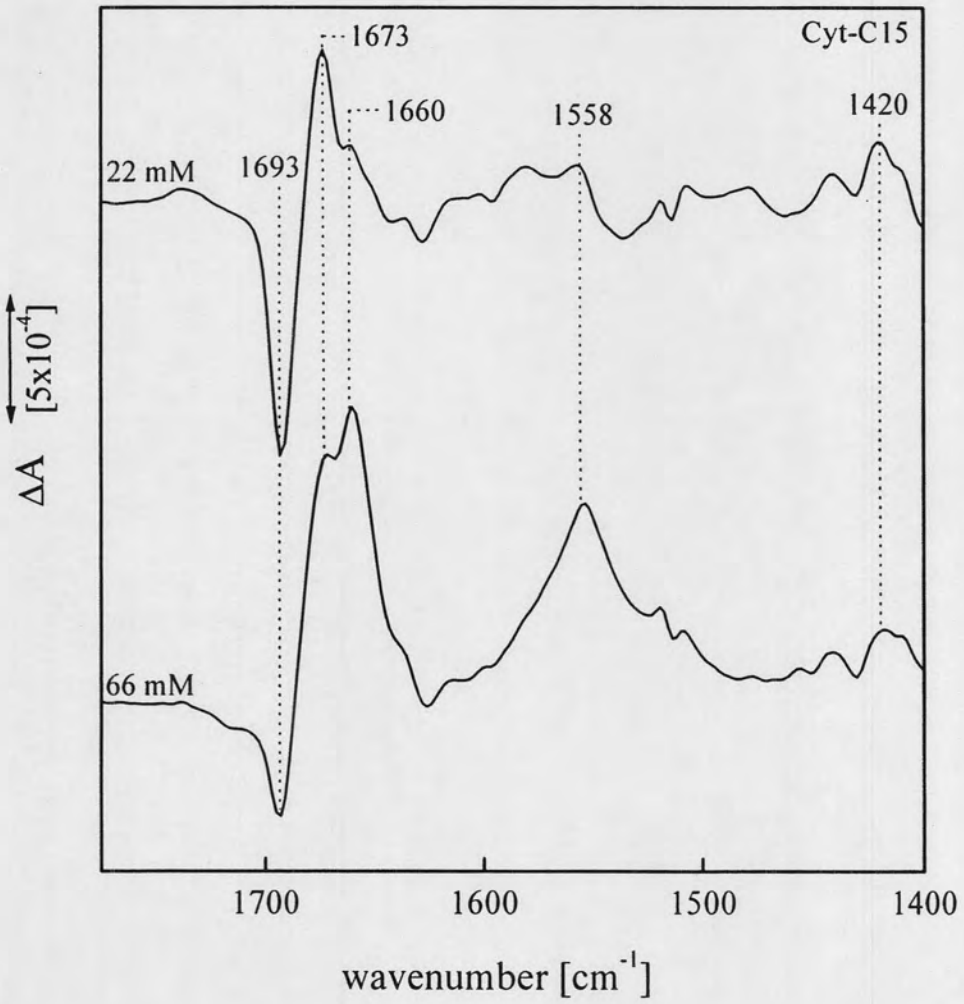

Figure 4.15 SEIRA difference spectra of Cyt-c immobilised on C15-SAM coated Au electrode at different ionic strengths (22 and 66 mM). The spectra of the oxidized (positive bands) and reduced state (negative bands) were measured at +0.1 and -0.1 V, respectively.

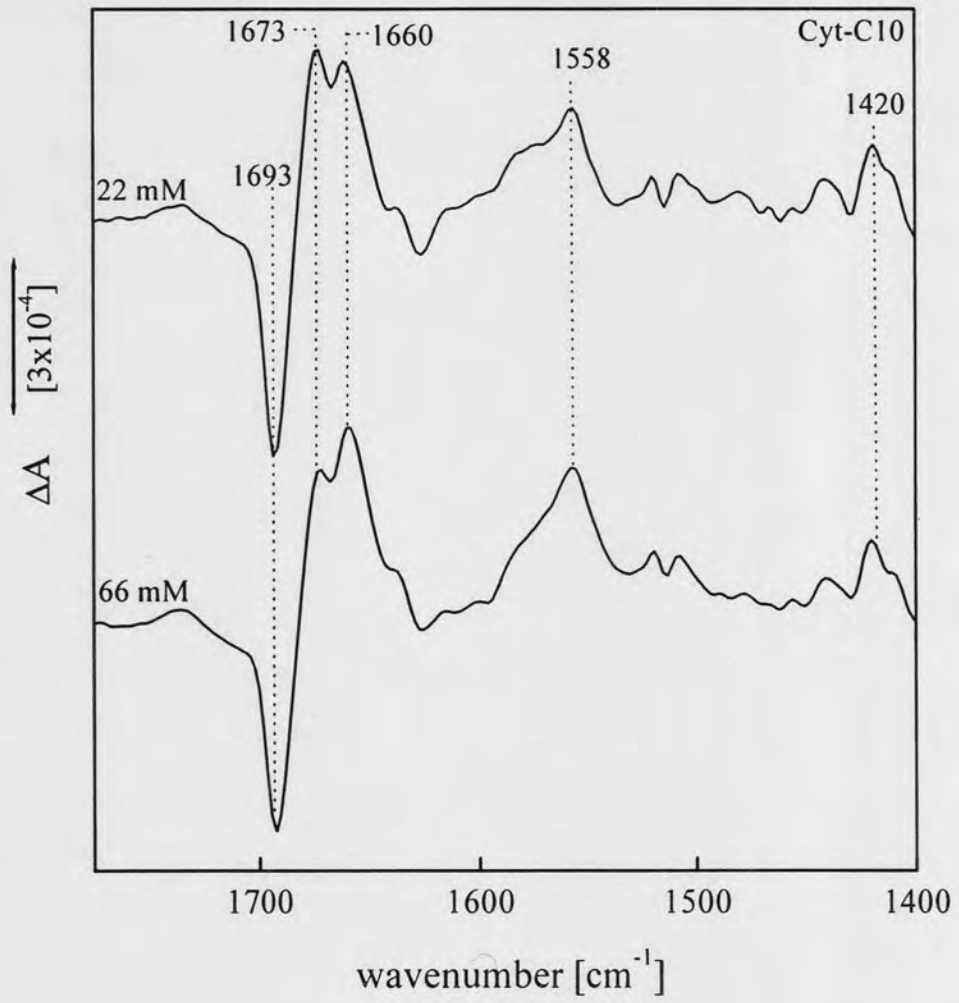

Figure 4.16 SEIRA difference spectra of Cyt-c immobilised on a C10-SAM coated Au electrode at different ionic strengths (22 and 66 mM). The spectra of the oxidized (positive bands) and reduced state (negative bands) were measured at +0.1 and -0.1 V, respectively.

On the first sight, the SEIRA difference spectra are quite different from the electrochemically induced IR difference spectrum of Cyt-c in bulk-solution, Figure 4.17. A careful inspection, however, reveals that most of the positive and negative bands are present in both spectra albeit with different relative intensities implying that the (secondary) structure and the structural details of the heme pocket are preserved upon adsorption [6,27,32]. The most striking exception refers to the 1666- and 1660-cm^{-1} bands in the SEIRA difference spectrum since they are not observed in the IR difference spectrum of Cyt-c in solution, which in turn displays a band pair at 1663

and 1651 cm^{-1}. It is tempting to assume that both band pairs originate from the same Amide I modes, suggesting an adsorption-induced structural change of the underlying peptide segments that leads to the frequency upshift in the reduced (+ 3 cm^{-1}) and oxidised (+9 cm^{-1}) forms. Moreover, this interpretation may support the assignment to an α-helix segment rather than to the β-turn type II [68,74].

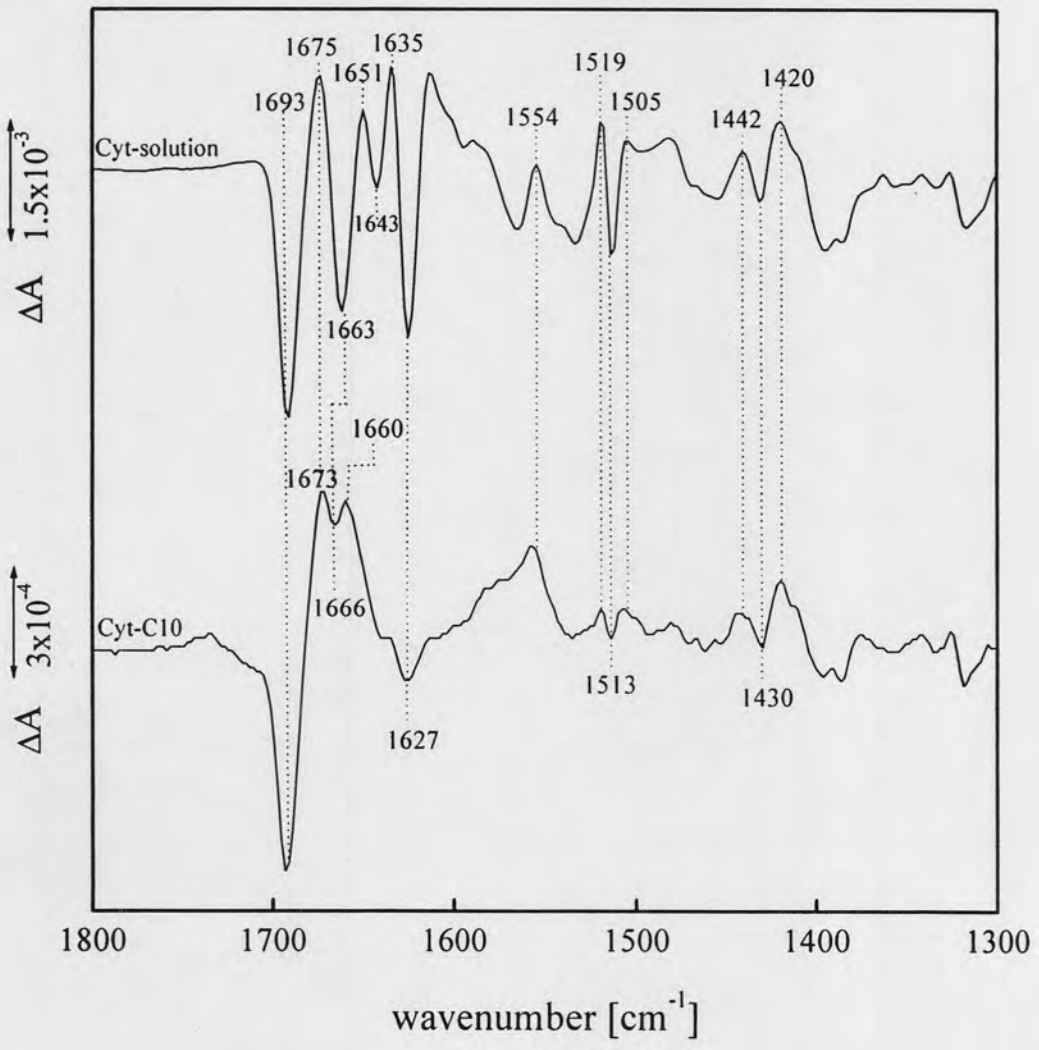

Figure 4.17 SEIRA difference spectrum of Cyt-c adsorbed on a C10-SAM coated Au electrode compared with the redox-induced IR difference spectrum of Cyt-c in solution. The spectra of the oxidized (positive bands) and reduced state (negative bands) were measured at +0.1 and -0.1 V, respectively. The experiments were carried out at an ionic strength of 22 mM (pH 7.0).

However, the 1693- and 1673-cm^{-1} band pair exhibits the same frequencies as observed in the redox-linked difference spectrum in solution. Thus, in this case, direct effects of the electrode potential that are redox-state independent can be ruled out and this band pair evidently reflects the same redox-linked structural changes of the β-turn III segment in the adsorbed state as in solution. These changes are likely to be very small and clearly beyond the level of secondary structure changes as in both cases the difference signals exhibit only 1–2% absorbance of the absolute band intensity suggesting the involvement of only one or two peptide bonds. In fact, Berghuis and Brayer [77] have demonstrated that redox-linked conformational changes of crystalline yeast iso-1 Cyt-c are restricted to small adjustments of the heme geometry, rearrangements of internal water molecules, and changes of thermal parameters of individual peptide segments. Among the latter are the residues 65–72, specifically Tyr67, which is consistent with the assignment of the 1693/1673-cm^{-1} band pair. The situation is different for the 1666/1660-cm^{-1} band pair which is shifted to higher frequencies as compared to the solution spectrum. These findings point to a structural change of the underlying peptide segment brought about by immobilisation.

In comparison to the difference spectrum of Cyt-c in solution, the SEIRA intensities of the Amide I bands depend upon the orientation of the peptide bonds with respect to the surface and a varying distance of the structural elements from the surface. This is due to the fact that Cyt-c is bound with a preferential orientation on the surface. If the intensity ratio of the conjugate peaks is similar as in solution, the redox transition will not be associated with an orientational change of the peptide segments involved. This appears to be the case for Cyt-c adsorbed on C15-SAM at low ionic strength and on C10-SAM independent of the ionic strength. At low ionic strength, the band pair at 1693/1673 cm^{-1} is the most dominant band implied that the β-turn type III is located close to the surface during the transformation from the reduced Cyt-c to the oxidized form [6]. In contradictory, at high ionic strength a drastic decrease of the 1693-cm^{-1} peak height and the increase of the 1673-cm^{-1} band intensity is found. This suggests a redox-state-dependent orientational change of the β-turn III segment 67–70 is involved in which this particular structural segment in the reduced form is located in a larger distance from the surface. Concomitantly, the intensity of the 1660-cm^{-1} band considerably increases on C15-SAM and, to a minor extent, also on C10-SAM upon

raising the ionic strength, implying a reorientation of the underlying peptide segment in the oxidized state. Independent of the ionic strength, a small peak intensity of the characteristic for an extended β-strand at 1635 and 1627 cm^{-1} in the oxidized and the reduced form, respectively, also reveals that the (backbones of) residues 37-40 and 57-79, which are found "above" the heme plane [6], are located in a further larger distance from the surface. These variations of the Amide band intensities most likely have a common origin: both the thickness of the SAM, i.e., the separation of Cyt-c from the electrode, and the ionic strength, which are the parameters controlling the electric field strength at the protein binding site [3,4,26], which in turn is likely to affect the orientation of individual peptide segments. Such orientational changes may either result from the alteration of the tertiary structure or from the reorientation of the entire immobilised protein (vide infra). Considering the heme vibration in the oxidized and reduced state at 1602 and 1595 cm^{-1}, respectively, they are clearly detectable in the SEIRA difference spectra independent of the ionic strength. Taking into account the SEIRA selection rules, a model in which Cyt-c binds to the SAM with the heme plane parallel to the surface can be neglected because the change of its dipole moment would not attribute to an enhancement. Moreover, it has been proposed that the heme plane is tilted by 46^{o} to the surface with a minor angular fluctuation ($\pm 6^{o}$) under the adsorption to the carboxyl-terminated SAM [78]. A similar orientation was also suggested from SERRS investigation, however, a certain orientation angle has not been specified by this method [79,80]. A tiny peak intensity is also found for the 1642-cm^{-1} band, which was assigned to an unordered structure of the reduced Cyt-c containing Met-80 and Phe-82. Met-80 is coordinated in the axial position to the heme, which is also located close to surface. The intensity decrease of this band may be caused by a change in the angle of the heme plane towards a more parallel orientation with respect to the surface. Similarly, a decrease of the peak intensities of the tyrosine (Try-48 and Try-67), compared to that of the solution spectrum, is found at 1519/1513/1505-cm^{-1}. This may be a reason of a re-orientation of the aromatic ring of (one of) the tyrosine residues to a more parallel alignment with respect to the surface.

4.2.3 Redox Potential of Native B1 Cytochrome c

A series of potential-dependent SEIRA difference spectra of Cyt-c adsorbed on C10-SAM using a spectrum measured at -0.1 V as a reference, is shown in Figure 4.18. A spectral difference between the two redox states is already present at -0.05 V, "positive" and "negative" peak intensities for the oxidized and reduced state raise with increasing electrode potential. As a result, the SEIRA difference signals may be ensured/derived from structural or orientational changes of the peptide segments, either induced by a variation of the electrode potential or the redox state change of the heme. At positive potentials ($\geq$+0.15 V), the intensities of the 1673- and 1660-cm^{-1} bands sometimes dropped as soon as a non-native species of Cyt-c is formed which always occurs at high electrode potentials (more detail will be discussed in next section) [29,31]. Measuring the SEIRA difference spectra as a function of the electrode potential allows the determination of the redox potential of the immobilised Cyt-c by fitting the experimental value to the Nernst equation. The intensities of the difference signals at 1673 and 1660 cm^{-1} (ferric Cyt-c) show a characteristic potential-dependence (Figure 4.19) that can be described by the Nernst equation yielding a redox potential of ca 0.03 and 0.05 V, respectively, i.e., a mean value of 0.04 V. The number of transferred electrons derived from the fit is close to the theoretical value of one. The redox potential determined in this way was found to be the same for other SAM lengths as well, i.e., C15-, C5-, C2-, and C1-SAM, and independent of the ionic strength within the experimental accuracy (± 10 mV) [81,82]. This value is only slightly more negative than the redox potential of Cyt-c in solution (ca. 0.06 V) [32,33]. The E^0 and n determined from the1673- and 1660-cm^{-1} band are always similar with those values after subtracting the spectral contribution of monolayer from the spectra of Cyt-c even for the short monolayer (C1- and C5-SAM), which have a large spectral contribution from the monolayer (vide supra). The difference in the E^0 determined from these two positive bands suggests the difference in the orientational behavior of these two peptide backbone during the transformation from the reduced to the oxidised Cyt-c.

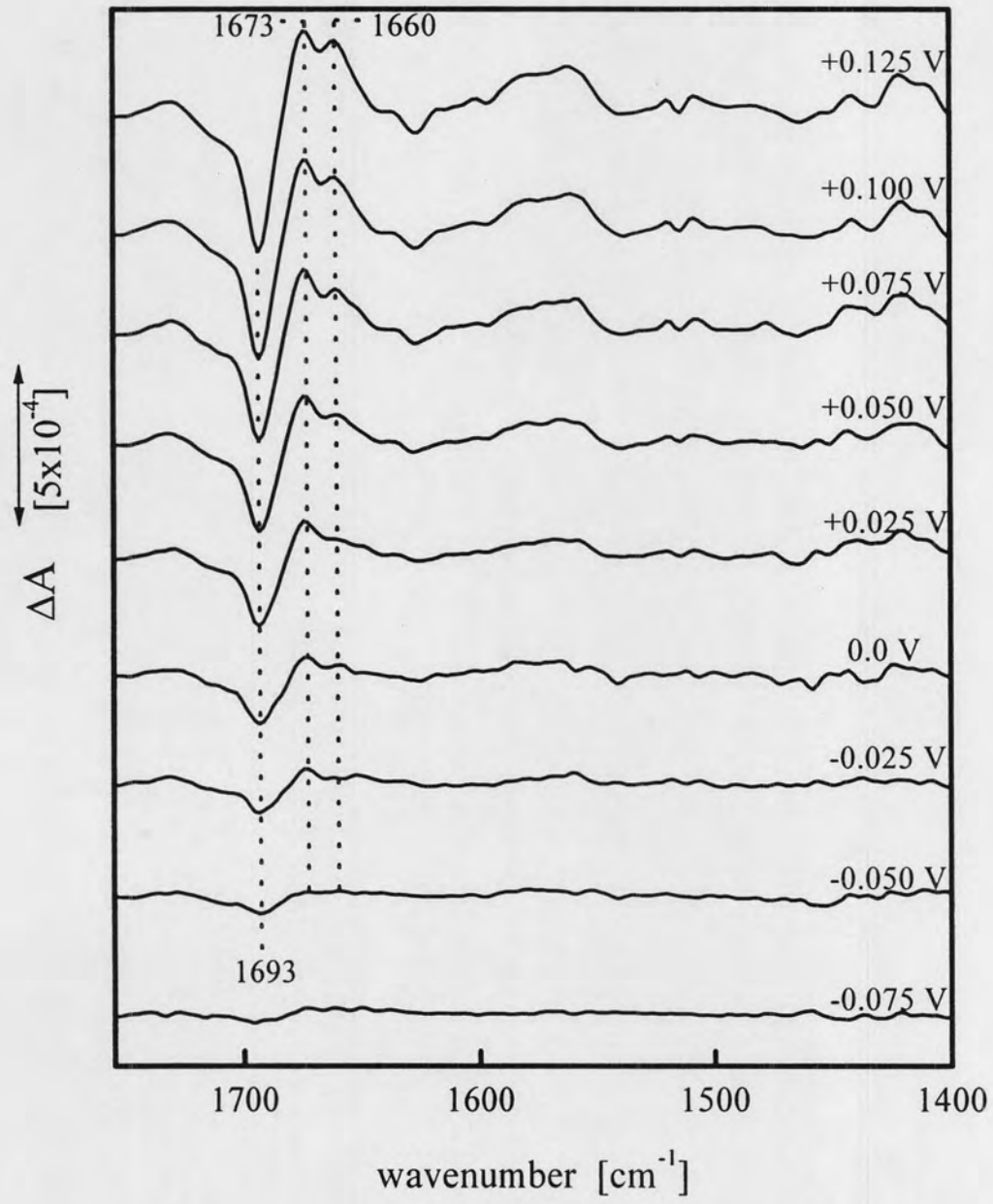

Figure 4.18 SEIRA difference spectra of Cyt-c adsorbed on a C10-SAM coated Au electrode, obtained as a function of potential. The reference spectrum of the reduced state was measured at -0.1 V. The experiments were carried out at an ionic strength of 66 mM (pH 7.0).

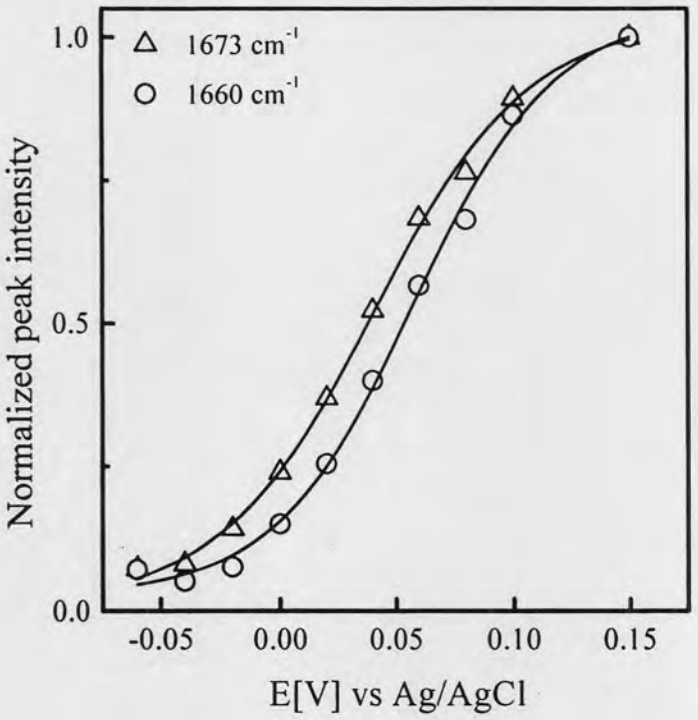

Figure 4.19 Potential-dependence of the peak height of the SEIRA difference bands at 1673 (triangles) and 1660 cm^{-1} (circles) as obtained from the potential-dependent SEIRA difference spectra. The solid line represents the fit of the Nernst equation to the experimental data.

Unlike those values, which are determined on the SAM coated Ag-electrode by the SERR-technique [26], a distance-dependence of E^0 is not observed for the values determined with the SEIRA method for Cyt-c adsorbed on the SAM coated Au-electrode. This might be related to the difference of the PZC, which is more positive for Au (ca. 0.40 V) [83] as compared to -0.70 V for the Ag [29,83-86]. Thus, for electrode potentials around the redox potential of Cyt-c, $\left[E - E_{pzc}\right]$ is negative for Ag but positive or close to zero for Au, corresponding to the larger electric field strength on Ag than on Au. This conclusion is consistent with the fact that the smaller potential-drop across the Au/SAM/Cyt-c interface, which is reflected by a shift in the redox potential, is much smaller than for the Ag system. The distance-independence of E^0 has also been observed by the investigations carried out with cyclo-voltammetry technique, which were also performed on SAM coated Au-electrodes [81,82].

4.3 Electric Field Induced Conformational Transition of the Immobilised Cytochrome c

To probe the spectral changes of the immobilised Cyt-c under an influence of EF strength, the potential-dependent SEIRA difference spectra were measured at various potential and at different monolayer chain lengths by using the SEIRA spectrum of -0.1 V as the reference. The relative intensity changes of SEIRA difference spectra are visualized by normalising the potential-dependent difference spectra with respect to the most distinguished negative band at 1693 cm^{-1}. Looking at various monolayer chain lengths, the difference spectra of the immobilised Cyt-c adsorbed on the carboxyl-terminated SAMs reveals always the same band frequencies, as shown in Figure 4.20. The overall amplitude of the SEIRA difference spectra decreases with shortening the monolayer chain length corresponding to an increase of the local EF strength. The normalized spectra of these difference spectra with respect to the 1693-cm^{-1} band are shown in Figure 4.21. The relative peak height, especially of the Amide I bands, decreases with decreasing SAM chain lengths. Although the relative peak height of most of the bands decreases with increasing the local EF strength, the 1642-cm^{-1} band which was assigned to an unordered structure, is more intense when Cyt-c adsorbed on the bare Au-electrode. It is in line with a more pronounce appearance of the heme vibrations at 1602/1595 cm^{-1}. Figure 4.22 displays the normalized potential-dependent SEIRA different spectra with respect to the 1693-cm^{-1} band measured at different potentials. The changes of relative peak height of Amide II and Amide III bands are about on the same level at each potential. However, the changes are largely found for the 1693-, 1673- and 1660-cm^{-1} bands. The plots of the peak heights of the 1673- and 1660-cm^{-1} bands of ferric Cyt-c with respect to the 1693-cm^{-1} band as function of potential for various monolayer chain lengths are shown in Figure 4.23. The relative peak heights of the β-turn III (1673 cm^{-1}) and β-turn II/α-helix (1660 cm^{-1}) of the ferric Cyt-c increase with raising electrode potential, however the relative peak height of the latter appear to increase faster. Whereas, the relative intensities of Amide II and Amide III bands change on the same level with respect to the 1693-cm^{-1} band independent of the electrode potential. The relative intensity changes of the β-turn III (1673 cm^{-1}) are very small when Cyt-c is adsorbed to C15-SAM as its relative intensities are almost the same for

each potential. Relative intensity changes of the immobilized Cyt-c is also found after an absorption of Cyt-c, on the bare Au-electrode covered with phosphate anions, was carried out at different fixed potentials, Figure 4.24. The potential-dependent SEIRA difference spectra were acquire immediately after Cyt-c was completely adsorbed on the electrode at open circuit potential which is always positive and at a negative potential of -0.20 V. The relative peak heights of Amide II and Amide III bands with respect to the band at 1693 cm^{-1} are not changed after Cyt-c absorption was carried out at different potentials. However, the relative peak heights of the β-turn III (1673 cm^{-1}) and β-turn II / α-helix (1660 cm^{-1}) backbone of the ferric Cyt-c was found to be decreased after the absorption of Cty-c was carried out at -0.2 V.

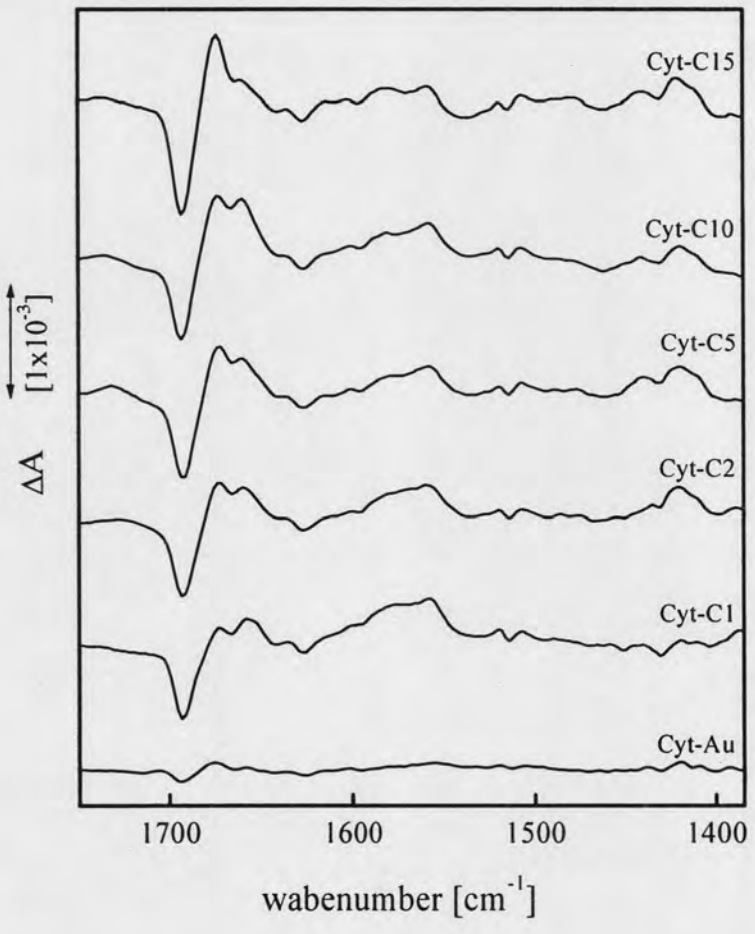

Figure 4.20 The SEIRA difference spectra of Cyt-c adsorbed on a Au-electrode and on SAM with various chain lengths. The spectra of the oxidized (positive bands) and reduced state (negative bands) were measured at +0.1 and -0.1 V, respectively. The experiments were carried out at an ionic strength of 22 mM (pH 7.0).

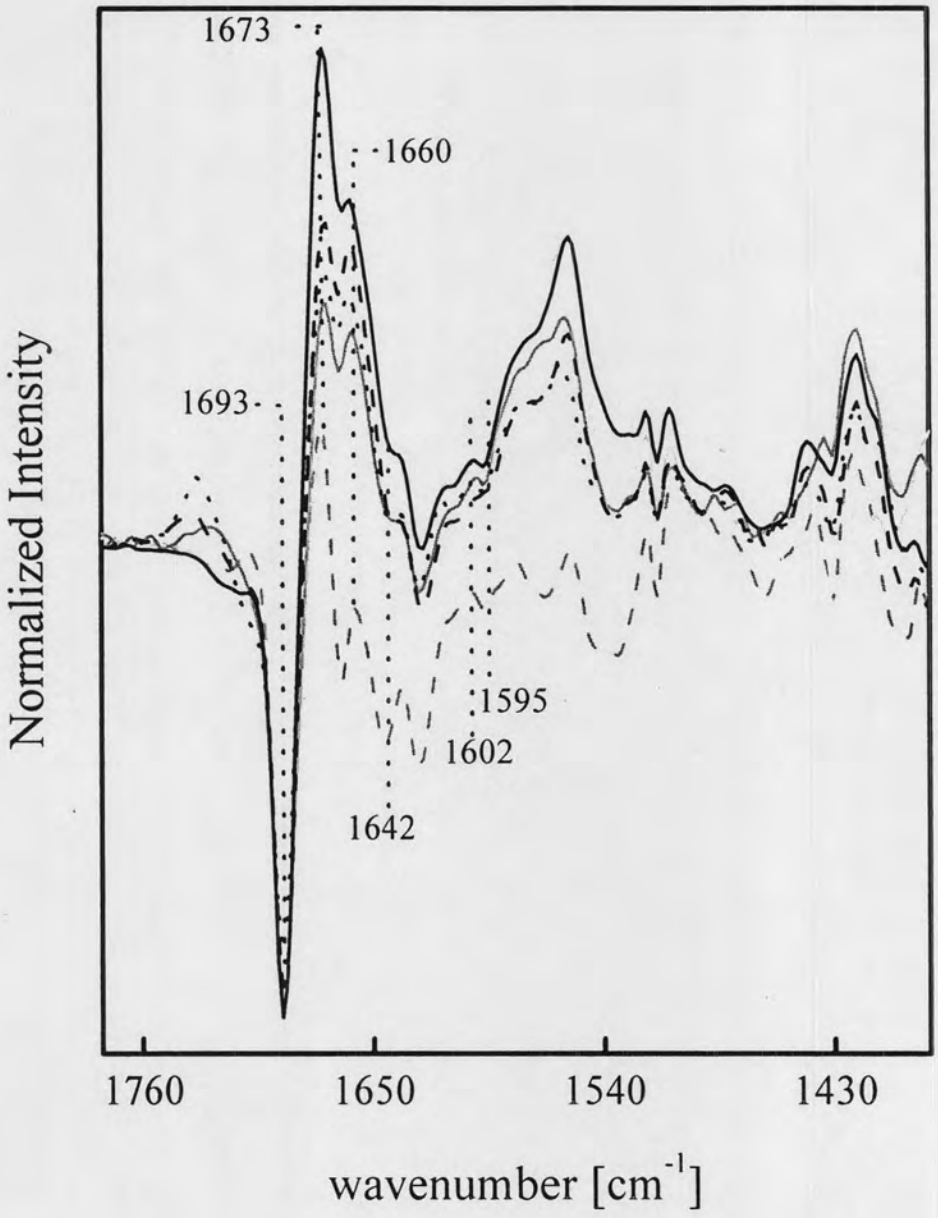

Figure 4.21 The normalized SEIRA difference spectra of Cyt-c adsorbed on a Au-electrode (gray, dash), and on C1- (light gray, solid), C2- (gray, solid), C5- (black, dot), C10- (black, dash) and C15-SAM (black, solid). The spectra of the oxidized (positive bands) and reduced state (negative bands) were measured at +0.1 and -0.1 V, respectively. The experiments were carried out at an ionic strength of 22 mM (pH 7.0).

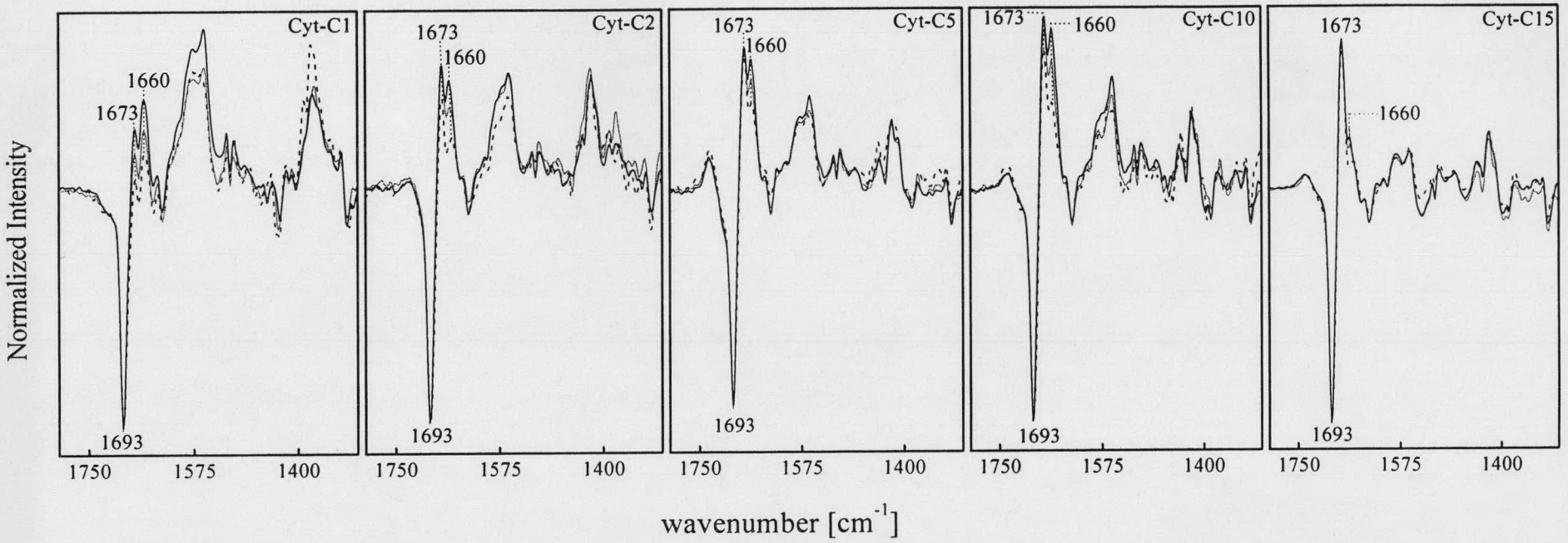

Figure 4.22 The normalized SEIRA difference spectra of Cyt-c adsorbed on C1-, C2-, C5-, C10- and C15-SAMs at selected electrode potentials; 0.0 (black, dash), +0.05 (gray, solid) and +0.10 V (black, solid). The reference spectrum was recorded at -0.10 V. The experiments were carried out at an ionic strength of 22 mM (pH 7.0).

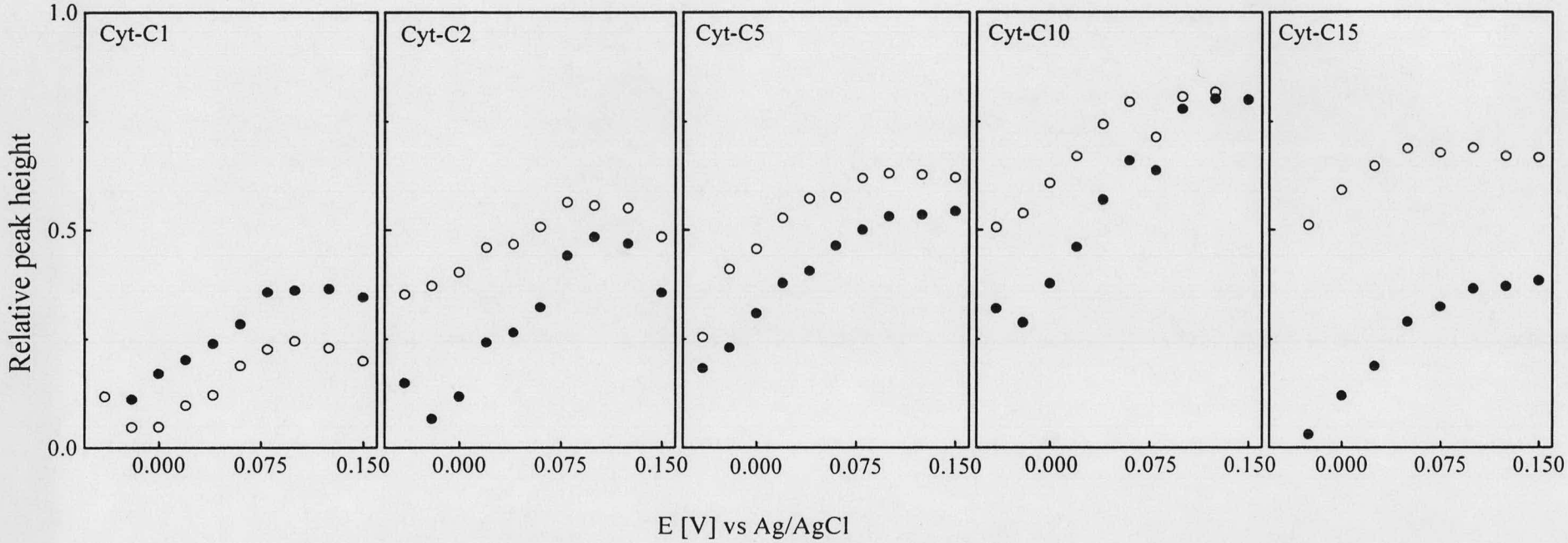

Figure 4.23 Plot of the relative band intensities of 1673 (circle, open) and 1660 cm^{-1} (circle, close) bands characteristic for the oxidized state relative to the band at 1693 cm^{-1} in the reduced state as a function of electrode potential for Cyt-c adsorbed on C1-, C2-, C5, C10, and C15-SAMs. The reference spectrum was recorded at -0.10 V.

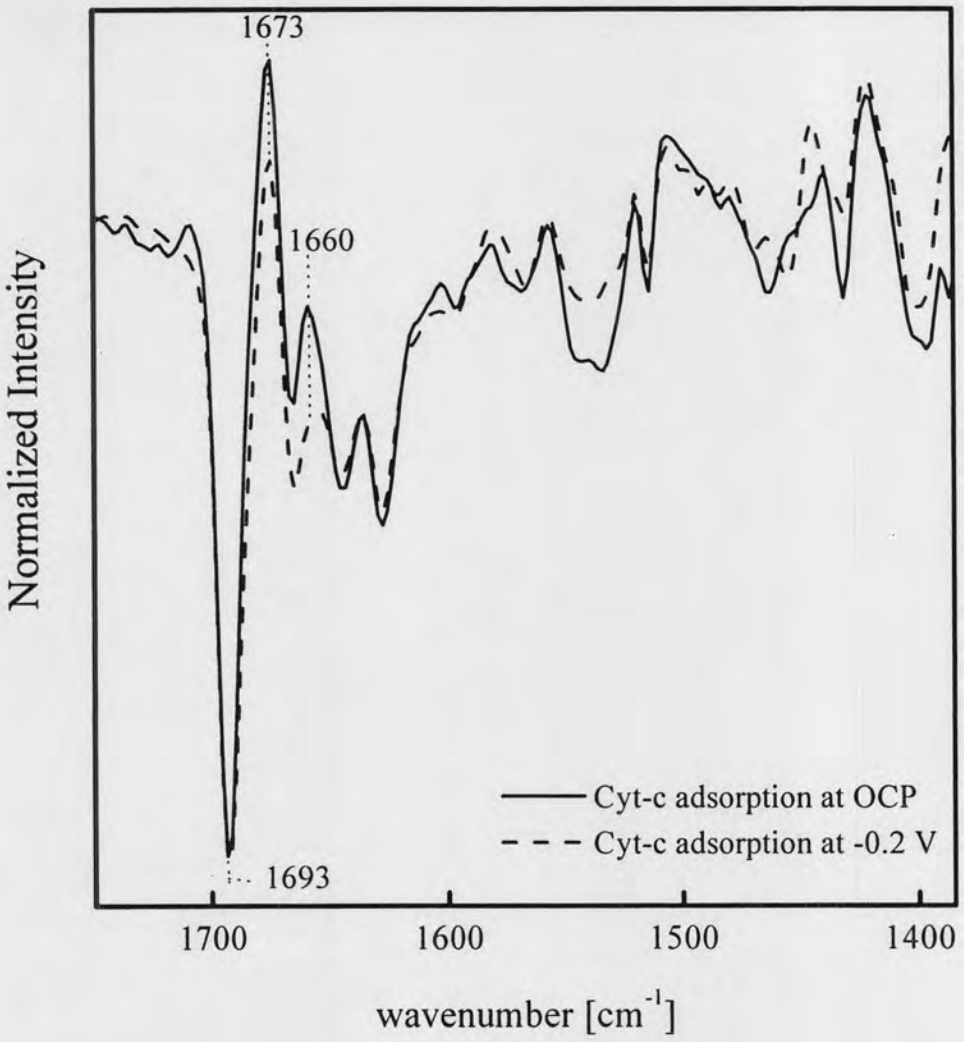

Figure 4.24 The normalized SEIRA difference spectra of Cyt-c adsorbed on a Au-electrode covered with phosphate anions after Cyt-c adsorption at OCP (sloid) and at -0.20 V (dash), with respected to the 1693-cm^{-1} band. The spectra of the oxidized (positive bands) and reduced state (negative bands) were measured at +0.1 and -0.1 V, respectively. The experiments were carried out at an ionic strength of 22 mM (pH 7.0).

The orientational changes of Cyt-c are linked with the changes of relative intensity of the difference spectra of Cyt-c, which is found to be correlated with the conformational transition from the native B1 to non-native B2 state of Cyt-c induced by the EF strength. In the present work, the EF strengths were controlled by varying the monolayer chain length and electrode potentials. The same band frequencies of

the difference spectra suggest an identical secondary structure of Cyt-c independent of the EF strengths. In fact, it was found that the formation of B2 Cyt-c does not involve the changes in the secondary structure but is associated with alterations of tertiary structure, which is involved in the dissociation of Met-80 and the movement of the peptide segment 30(20) - 49 to bring either His-33 or His-26 in proximity to the heme. The transition from the B1 to B2 state is found to be involved in the orientational changes of β-turn III (1673 cm^{-1}) and β-turn II/α-helix (1660 cm^{-1}) in the oxidized form, as well as the reduced form of β-turn III (1693 cm^{-1}) segment. Within the potential range between -0.1 V and +0.1 V, Cyt-c is predominant in the B1 state. Gradually increase of the potential from -0.1 V to +0.1 leads to the orientation of those three segments of Cyt-c, therefore the relative intensities of the 1673- and 1660-cm^{-1} bands are increasing with raising the potential in which the relatively weaker EF strength with respect to the pzc is induced at more positive potential. In contrast, the re-orientation of Cyt-c at more negative potentials, where the EF strength is relatively strong, will induce the transformation of Cyt-c from the B1 to the B2 state. The β-turn type II/α-helix structure of the oxidized Cyt-c (1660 cm^{-1}) seems to be more sensitive to the EF than that of the β-turn type III (1673 cm^{-1}) in the oxidized form as its relative peak intensity increases much faster with increasing the electrode potential. Considering the Cyt-c adsorbed on C15-SAM where no B2 is found, the EF is too weak to induce the orientational changes of the oxidized β-turn III as reveal by the small changes of relative intensity of the 1673-cm^{-1} band as function of potential. In contrary, changes in the relative intensity this band is more pronounced at strong local EF strength (C1-SAM).

Relative orientational changes of the β-turn III (1673 cm^{-1}) and β-turn II/α-helix (1660 cm^{-1}) segments of the oxidized Cyt-c are also revealed when Cyt-c was adsorbed on the bare Au-electrode at a fixed potential, i.e., at -0.2 V and at the open circuit potential. For the same reason, the relatively high EF strength generated at the potential of -0.2 V, induces the transformation from the native B1 to the non-native B2 state of Cyt-c upon the re-orientation of the β-turn type III (1673 cm^{-1}) and α-helix III (1660 cm^{-1}) segments of ferric Cyt-c as demonstrated by a decrease of their relative intensities. This is in contrast to a result obtained for Cyt-c on Ag-electrode where the adsorption at the potential of -0.2 V leads the formation of the B1 Cyt-c

while the B2 state is preferentially formed when the adsorption takes place at open circuit (ca. 0.0 V). This discrepancy can be understood in terms of the potential difference $|E_{pzc} - E|$ with respect to the pzc since the potential difference decreases from "open circuit" to -0.2 V on Ag, but increases on Au concomitantly, which induces the stronger EF strength on Au than on Ag.

As the EF strength induced by SAM-length is stronger than that induced by the electrode potential for the Au electrode, the changes of relative intensity of Amide II and Amide III bands are more pronounced at a variation of the monolayer chain lengths, although the changes are insignificant. It was reported that the total amount of the B2 species is proportional to the local EF strength upon which Cyt-c was adsorbed on the carboxyl-terminated SAM. While no B2 Cyt-c is observed at C10-SAM, and its amount increases up to 75% at C1-SAM [31]. A decrease of the overall amplitude of the potential-dependent difference spectra with shortening monolayer chain length is established to be correlated with orientational changes of the β-turn III (1673 cm^{-1}) and the α-helix/β-turn II (1660 cm^{-1}) of ferric Cyt-c, as well as the reduced form of the β-turn III (1693 cm^{-1}) segment under the influence of the EF strength. A decrease of relative intensity of the 1673- and 1660-cm^{-1} bands of the oxidized Cyt-c with decreasing the SAM chain length can be explained by an increase of the amount of B2 with increasing local EF strength in correlation to the movement of His-33, which is presumably a part of β-turn II structure (1660 cm^{-1}), that induces the reorientation of the oxidized form of β-turn III (1673 cm^{-1}) and the α-helix/β-turn II (1660 cm^{-1}) structures during the formation of B2. At the bare Au-electrode where B2 species is prevalent, re-orientation of an unordered structure (1642 cm^{-1}) including the residues 79-81, is obviously pronounce than at the other SAM length. Relative orientational changes of this segment in Cyt-c is found to be correlated with the relatively changes of the heme of the 1602/1595 cm^{-1} band pair suggesting the part of Cyt-c that is close to the redox active center is destabilized by the strong local EF strength. This can be explained by the dissociation of Met-80 from the heme-pocket, which influences also a rearrangement of hydrogen-bonds around the heme.

4.4 Non-Native B2 Conformation of Cytochrome c

It has been known that the formation of the non-native B2 state of Cyt-c is induced by electric field strength and dependent on the interaction at the protein binding site, i.e., the hydrophobic and electrostatic interaction [27,31]. The characterization of the non-native Cyt-c was carried out by various spectroscopic techniques [27,28]. However, up to now the characterization of the B2 state using the SEIRA spectroscopy with its advantage of probing the whole backbone of the immobilized protein has not been performed. In this work, the SEIRA technique was carried out to examine the B2 conformation of Cyt-c after electrostatic attachment to the Au-electrode covered with phosphate anions.

4.4.1 Conformational and Redox Equilibria between the Native and non-Native State of Cytochrome c

To investigate the structural transition of Cyt-c, the potential-dependent SEIRA difference spectra of Cyt-c on the bare Au-electrode was carried out in the potential range between -0.5 to +0.15 V. The measurements were operated under an equilibrium condition to have an abundance of B2 structures using the SEIRA spectrum measured at a very negative potential of -0.5 V as the reference, Figure 4.25. Within this potential range, one should observe mainly the non-native B2 structure of Cyt-c, in which three redox transitions are revealed. The formation of the B2 species influences changes in the tertiary structure together with an arrangement of the hydrogen-bonding interaction as revealed by a broad and complex band of the SEIRA difference spectra resulting from several overlapping bands [27,29]. The previous results by Heimburg et al. and recently Bernard et al. also showed that changes of secondary structure of Cyt-c upon binding to an anionic lipid membrane are very small, but it largely contributes to changes of the tertiary structure [87]. If the secondary structure of a protein changes, the IR frequency of the peptide backbone will be shifted by ca. 8-10 cm^{-1} [24]. The waiting time to reach the equilibrium state at a negative potential is longer than at a positive potential, due to the fact that structural changes of Cyt-c are slower when the non-native B2 Cyt-c is formed.

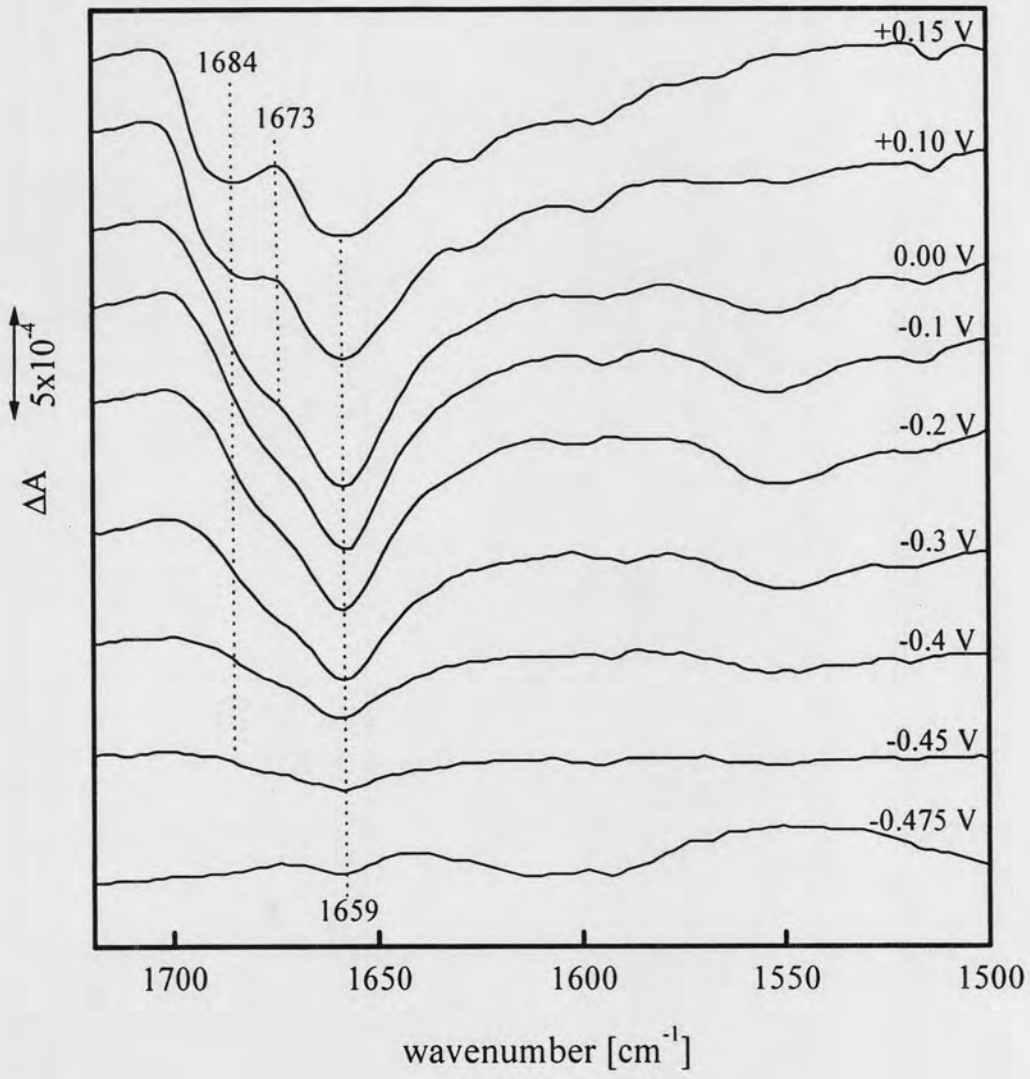

Figure 4.25 A series of the potential-dependent SEIRA difference spectra of Cyt-c adsorbed to the bare Au-electrode measured at the potential of -0.475, -0.45, -0.4, -0.3, -0.2, -0.1, 0.0, 0.1 and 0.15 V, respectively. The reference spectrum was recorded at -0.5 V. Spectra were measured in the equilibrium state.

To investigate the redox transitions of various states of Cyt-c, sigmodial curves incorporating the Nernst equation were fitted to the potential-dependent SEIRA intensity changes of the 1659-cm^{-1} band, which is the most dominated negative band of the reduced Cyt-c, Figure 4.26. Redox potentials (E^0) of -0.41 and 0.05 V were

revealed to be the values for the B2[6cLS] and B1[6cLS] corresponding to the number of transferred electrons of 1.08 and 1.2, respectively. The negative shift of E^0 of the B2 conformation compared to that value of the B1 state is due to the changes of the ligand pattern and the heme-pocket structure [29]. However, E^0 of the B1 state is always similar to the value of the solution. Due to experimental limitations, i.e., long equilibrium time at negative potential as well as the denaturation effects, the number of accessible data points was restricted. Therefore, an evaluation of the B2[5cHS] is ambiguous. In relation to the previous obtained SERRS results on a Ag-electrode for yeast iso-1 Cyt-c reported by Wacherbarth, for which the potential-dependent structural changes are expected to be similar for the horse heart (hh) Cyt-c [31], the redox potentials determined by SEIRA method are similar to those values obtained by SERR on Ag-electrode although the pzc of the metal electrodes are different.

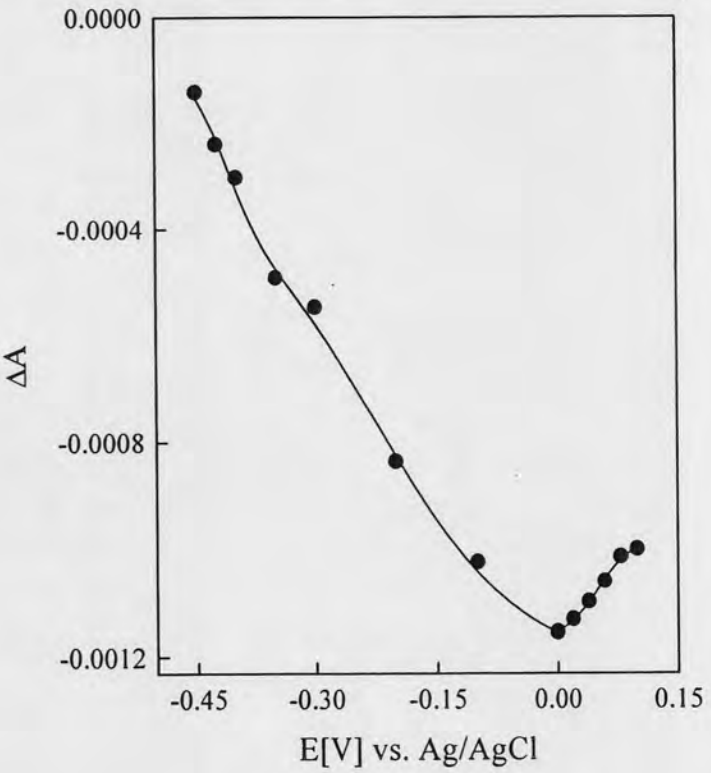

Figure 4.26 The potential-dependent peak intensities of the 1659-cm^{-1} band of Cyt-c immobilized on the bare Au-electrode covered with phosphate anions. The redox couples of Cyt-c are fitted to the summation of three Nernst functions represented by the continuous line. The reference spectrum was recorded at -0.5 V. The spectra were measured in the equilibrium state.

4.4.2 Characterization of the non-Native B2 Conformation of Cytochrome c

When Cyt-c is adsorbed on the bare Au-electrode, the formation of B2 species is induced, Figure 4.27c, d. Denaturation of Cyt-c is also caused by a direct attachment of proteins to the metal surface. Imperfect coverage of the SAMs on the metal electrode also induces the denaturation of Cyt-c since it can bound directly to the surface via a defect cover part of SAMs. A comparison of the SEIRA difference spectra of the B1, B2 and denaturated Cyt-c is shown in Figure 4.27. When Cyt-c is adsorbed on the bare Au-electrode with an applied electrode potential of -0.3 V in the equilibrium state, the non-native B2 species are prevalent, Figure 4.27d. The SEIRA difference spectra of denaturated Cyt-c reveal characteristic bands of the B1 and a small attribution of the B2 spectrum. Although these bands are characteristics for the secondary structures of Cyt-c, the structures are already deformed during the denaturation as their SEIRA signals are lost. (More details about characterization of B2 will be discussed below.) At potentials below -0.1 V, although there is also a contribution of the B1 state of Cyt-c on the bare Au-electrode, which is already fully reduced at a potential of -0.1 V [6,31,32]. Thus, the reduced B1 state of Cyt-c should not account for any spectral change in the difference spectra when the applied electrode potential lies below -0.1 V.

To elucidate the difference between the B1 and B2 conformation and to identify characteristic SEIRA band frequencies for the B2 species, the difference spectra of Cyt-c in solution and the one of Cyt-c adsorbed to the bare Au-electrode acquired at -0.30 V are utilized, Figure 4.28a and b. Under the latter condition, the B2 species are prevalent. In such a way, the difference spectrum measured with the potential of -0.3 V can be used as the characteristic spectrum for B2 states compared to the spectrum of Cyt-c in bulk solution where only the B1 state is formed. The corresponding 2^{nd}-derivative of the difference spectra displayed in Figure 4.29 reveals the following: When the B2 state prevails, changes of the tertiary structure and hydrogen-bonding interactions induce the broad band overlaps of the Amide mode. Only a few amide I bands can be distinguished resolved and no changes of the reduced form of β-turn III (1693 cm^{-1}) are found, as indicated by the absence of this band. The band of the β-turn III (1673 cm^{-1}) of the ferric Cyt-c, which is always intense in the spectrum of B1,

is also less pronounced. The reduced-forms of the protein segments are more pronounced than the oxidized-forms compared to the B1 state, Figure 4.28a and b. A characteristic peak at 1680 cm^{-1}, which was assigned to a turn structure, is not detected in the spectrum of B1. The 1660-cm^{-1} band, which is always dominant in the B1 state in the oxidized form, is predominant in the B2 state in its reduced form. This might be due to a movement of the α-helix/β turn II in the reduced state presumably including His-33 to coordinate with the heme pocket. A broad negative band of the β-turn III around 1550 cm^{-1} band is found only at the potential below the redox potential of B1 state (≤ 0 V), where the B2 species are expected to be dominant (Figure 4.25). With potentials above the redox potential of the B1 state, both B1 and small amount of B2 species are found on the bare Au-electrode, Figure 4.28c and 4.29c.

Some of the detected bands, i.e. at 1673 and 1660 cm^{-1}, are slightly shifted in their positions compared to that of Cyt-c in solution. These bands also reveal the re-orientational and conformational changes between the B1 and B2 state under EF strengths (Chapter 4.2.5). The amide I mode of the 1693-cm^{-1} band (reduced β turn III), which is not present at potentials below the redox potential of the B1 state where B2 is prevalent, overlaps with the 1680-cm^{-1} band (turn segment), Figure 4.28. When both B1 and B2 Cyt-c are formed (Figure 4.29c), a decrease of the peak intensity for the unordered structure of the 1645-cm^{-1} band presumably including the residues 79-81 is observed, accompanied by a band shift to a lower wavenumber at 1643 cm^{-1}, which overlaps with the 1659-cm^{-1} band. This can be explained by the dissociation of Met-80 from the heme-pocket that influences also a rearrangement of hydrogen-bonds around the heme. Such a broad band is clearly detectable in comparison with the spectrum in solution. It may be due to a rearrangement of hydrogen-bonds involving the three segments of α-helix/β-turn type II (ca. 1659 cm^{-1}) and unordered (ca. 1645 cm^{-1}) structures, which include the important residues, i.e., His-33 and Met-80 respectively, for the formation of non-native B2 conformation of Cyt-c.

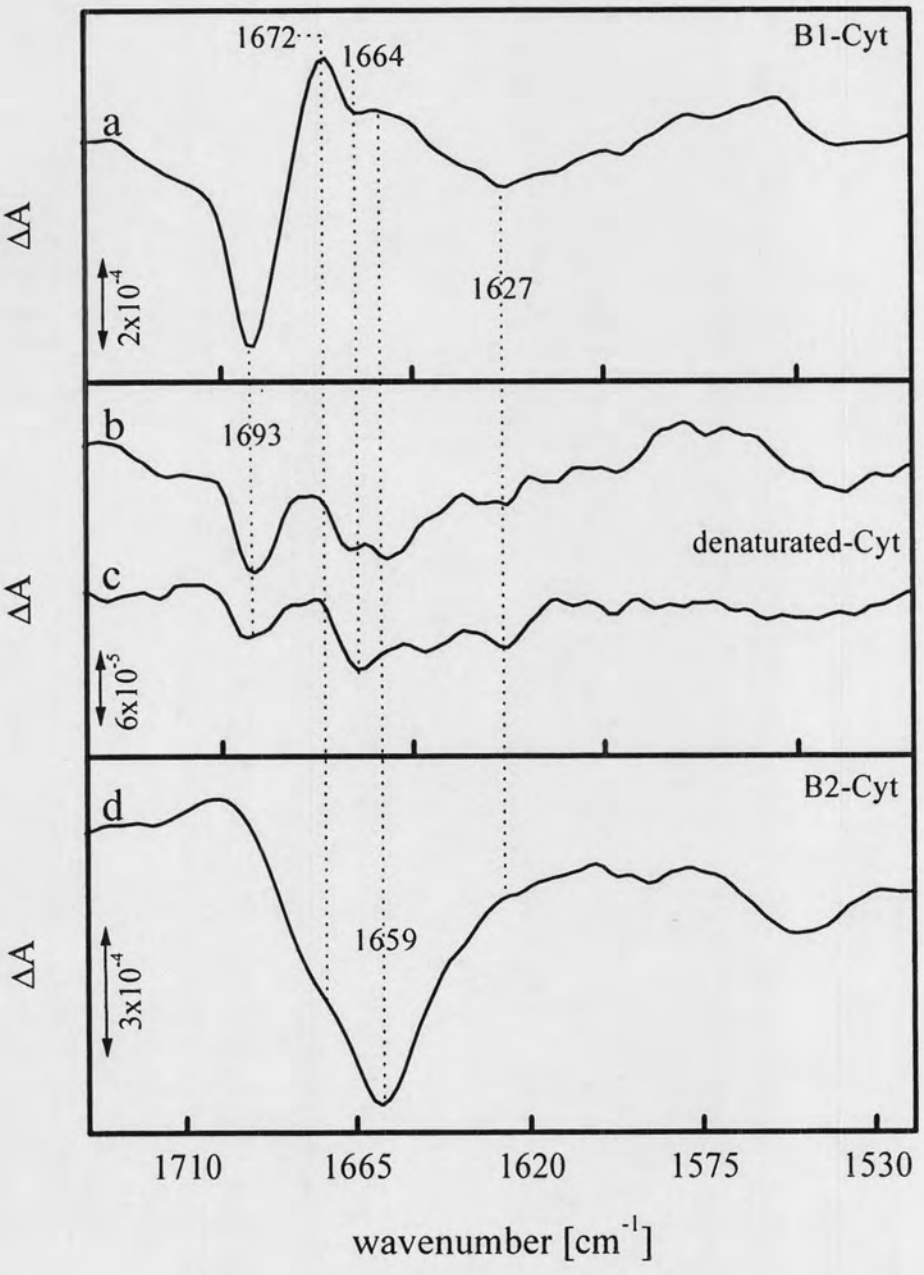

Figure 4.27 The potential-dependent SEIRA difference spectra of Cyt-c adsorbed to: C5-SAM measured at a potential of +0.02 V (-0.10 V as reference) with (a) a "perfect" and (b) non-perfect coverage of the SAM, and adsorbed to the bare Au-electrode measured at a potential of (c) 0.0 V (-0.1 V as reference) and (d) -0.30 V at equilibrium state (-0.5 V as reference).

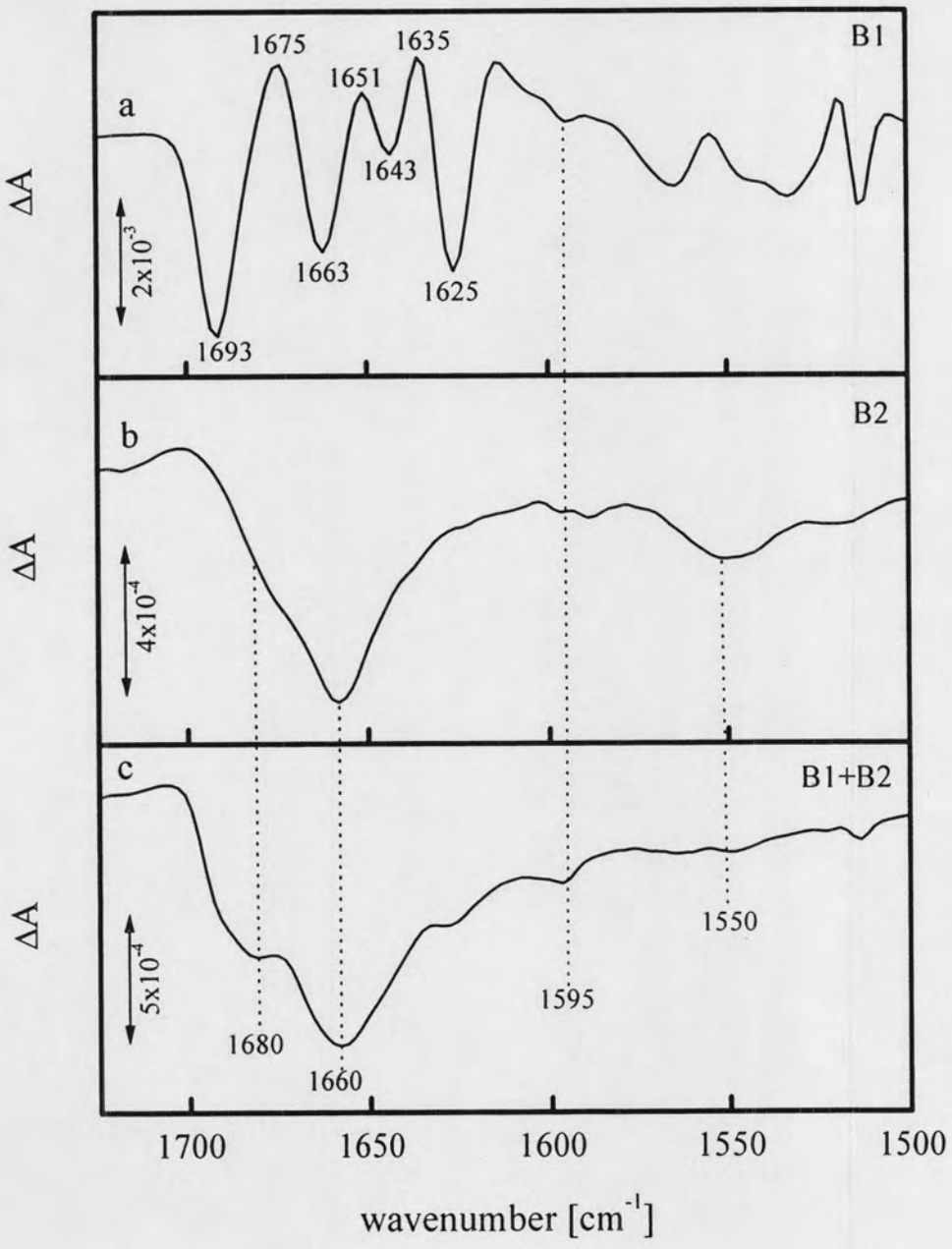

Figure 4.28 The potential-dependent SEIRA difference spectra (ox. minus red.) of Cyt-c in bulk solution (a), and adsorbed to the "bare" Au-electrode covered with phosphate anions measured at -0.30 V (b) and +0.10 V (c) using the spectrum at -0.50 V as reference. The measurements of the bound state were done under equilibrium conditions.

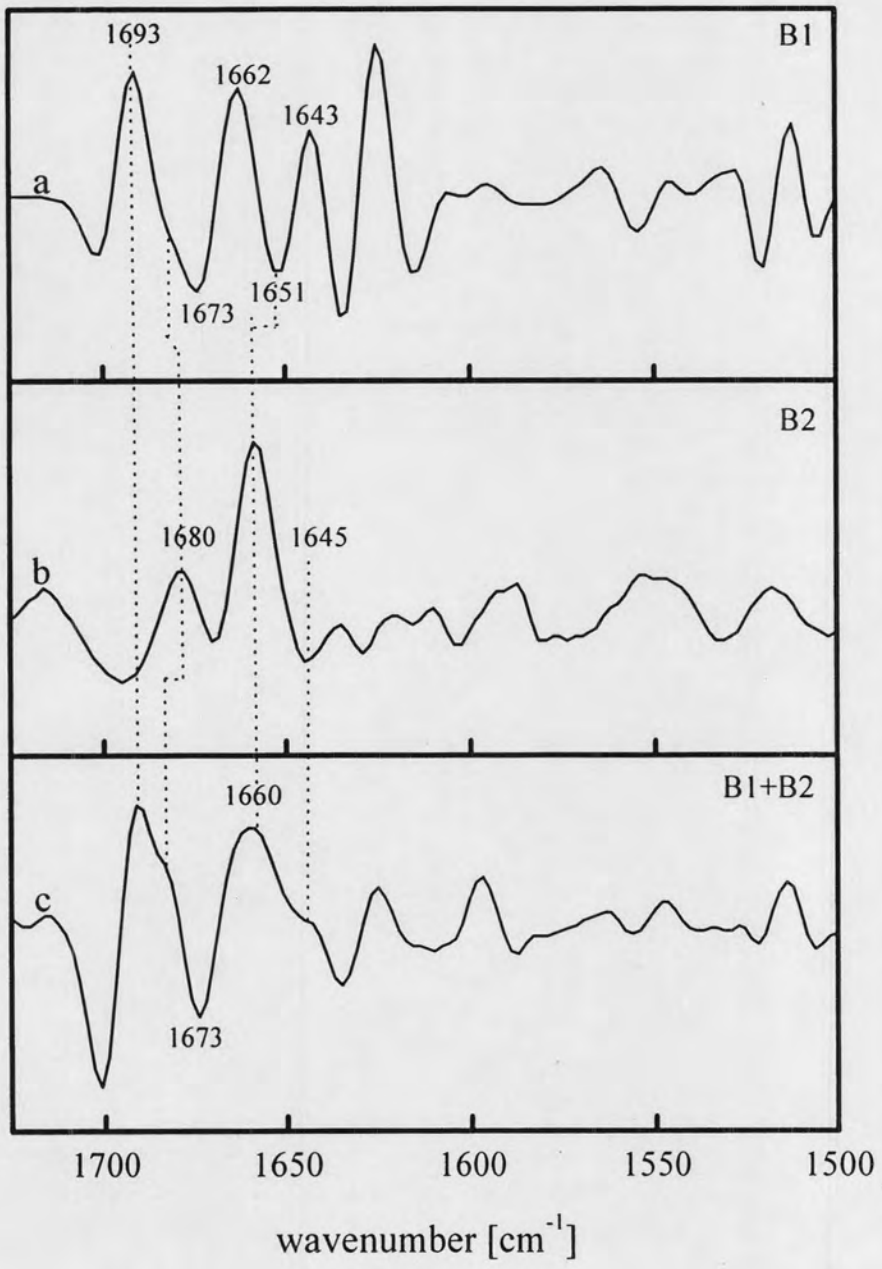

Figure 4.29 The 2nd-derivative spectra of potential-dependent SEIRA difference spectra (ox. minus red.) of Cyt-c in bulk solution (a), and adsorbed to the "bare" Au-electrode covered with phosphate anions measured at -0.30 V (b) and +0.10 V (c) using the spectrum at -0.50 V as reference. The measurements of the bound state were done under equilibrium conditions.

4.5 Time-Resolved SEIRA Spectro-Electrochemistry

To probe the electron transfer dynamics of the immobilized Cyt-c, rapid potential jumps were applied to perturb the equilibrium at the initial potential E_{ref}. The subsequent relaxation processes that establish the equilibrium at the final potential E_f, were monitored by time-resolved SEIRA spectroscopy probing the temporal evolution of the bands at 1693 cm^{-1} (ferrous Cyt-c) and 1673 and 1660 cm^{-1} (ferric Cyt-c).We have chosen E_{ref} to be -0.1 V and E_f was set equal to the redox potential E^0 (+0.04 V). For C15-SAM, the spectral changes were found to occur on the time scale of seconds which is appropriate to be probed by rapid-scan measurements, Figure 4.30. For each band, the time-dependent intensity changes can be well described by a mono-exponential kinetics with relaxation times (τ) that corresponds to a reciprocal relaxation constant $\left(k_{prot}\right)^{-1}$, Figure 4.32. The analysis reveals a relaxation constant of ca. 0.40 and 0.20 s^{-1} for the 1693- and 1660-cm^{-1} band, respectively (Table 4.1). Whereas the kinetics derived from these bands is independent of the ionic strength, the relaxation constant describing the intensity changes of the 1673-cm^{-1} band decreases from 0.40 s^{-1} at low ionic strength to 0.20 s^{-1} at high ionic strength. This finding is consistent with the ionic strength dependence of this band observed in the stationary SEIRA difference spectra (vide supra). At C10-SAM, the spectral changes occur with much faster rates such that the step-scan technique is employed for the kinetic analysis Figure 4.31. In this case, similar relaxation rate constants (75–90 s^{-1}) are obtained for the 1693- and 1673-cm^{-1} bands, regardless of the ionic strength. Again a smaller value is obtained (ca. 50 s^{-1}) for the 1660-cm^{-1} band. Whereas for both C15- and C10-SAMs, the error of the kinetic constants determined from the SEIRA experiments is estimated to be lower than 20%, step-scan measurements of Cyt-c on C5-SAM are associated with a larger uncertainty. Most likely, the lower stability and the higher structural heterogeneity of C5-SAM are the main reasons for the substantially stronger scattering of the kinetic constants in the individual measurements. Thus, the error is estimated to be two times larger than for C10- and C15-SAMs, i.e., ca. 40%. However, the results unambiguously indicate a further acceleration of the relaxation processes. The average relaxation constants that are derived from the intensity changes of the 1693-, 1673-, and 1660-cm^{-1} bands are

determined to be of 900, 700, and 600 s^{-1}. Within the experimental error, these values were found to be the same at an ionic strength of 66 and 130 mM. Note that at these ionic strengths the response time of the SEIRA electrochemical cell was better than 400 μs.

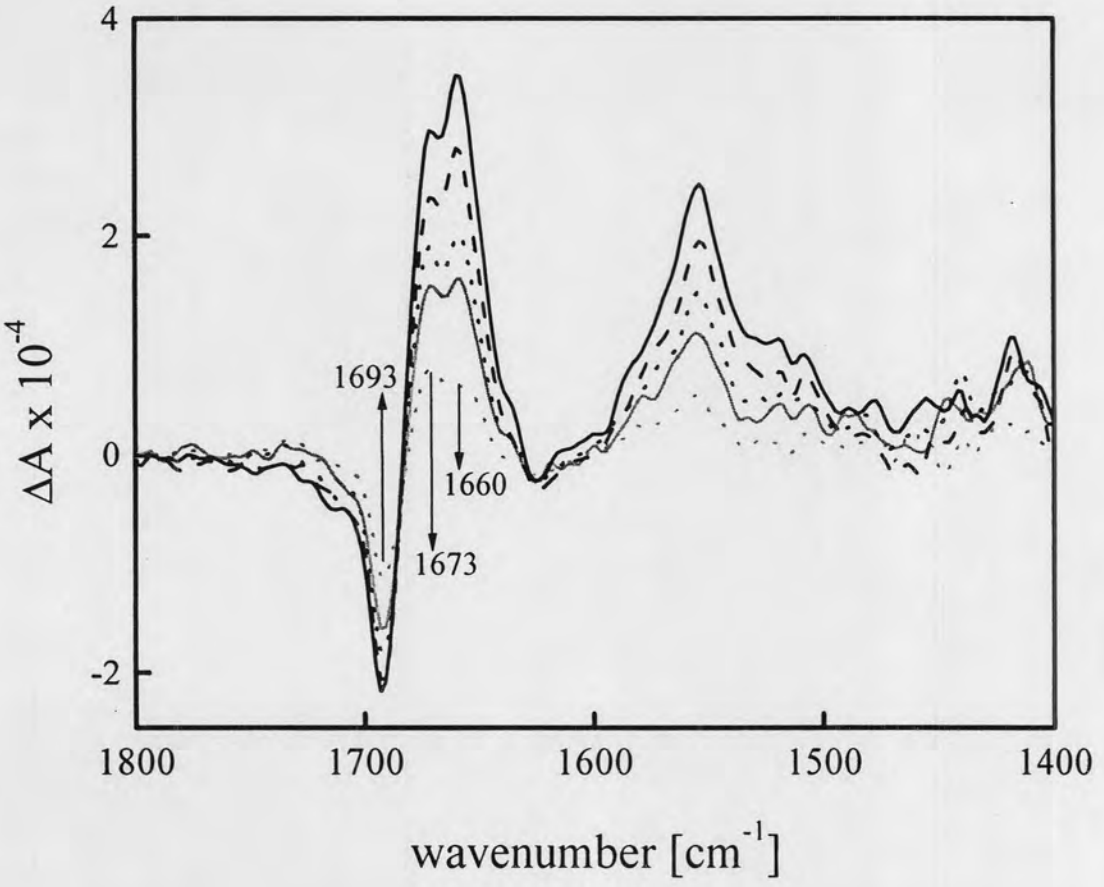

Figure 4.30 Rapid-scan SEIRA difference spectra of Cyt-c on C15-SAM coated Au electrodes using the spectrum measured at -0.1 V as a reference. The individual traces represent the difference spectra obtained at 1 (gray, dotted), 3 (gray, solid), 5 (black, dotted), 10 (black, dashed), and 20 (black, solid) s after the potential jump from -0.1 V to the redox potential (+0.04 V). The experiments were carried out at an ionic strength of 66 mM (pH 7.0).

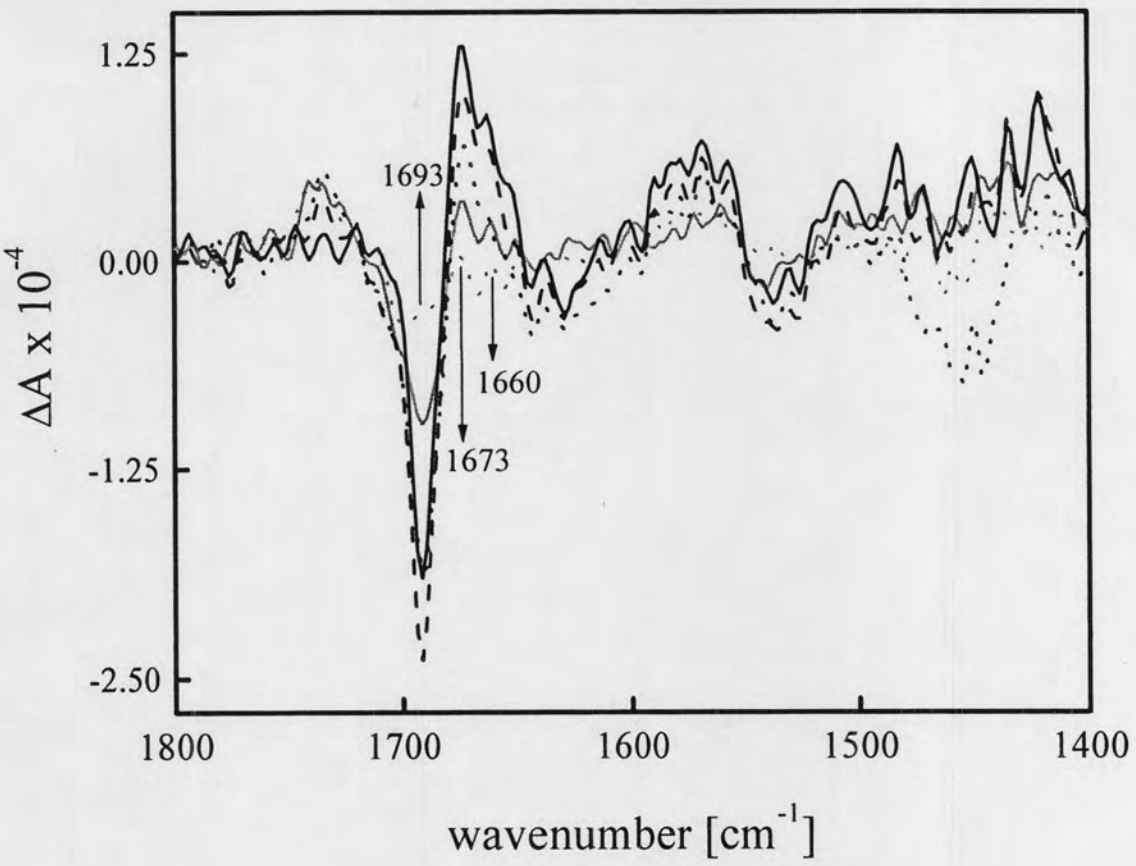

Figure 4.31 Step-scan SEIRA difference spectra of Cyt-c on C10-SAM coated Au electrodes using the spectrum measured at -0.1 V as a reference. The individual traces represent the difference spectra obtained at 5 (gray, dotted), 10 (gray, solid), 20 (black, dotted), 40 (black, dashed), and 70 (black, solid) ms after the potential jump from -0.1 V to the redox potential (+0.04 V). The experiments were carried out at an ionic strength of 66 mM (pH 7.0).

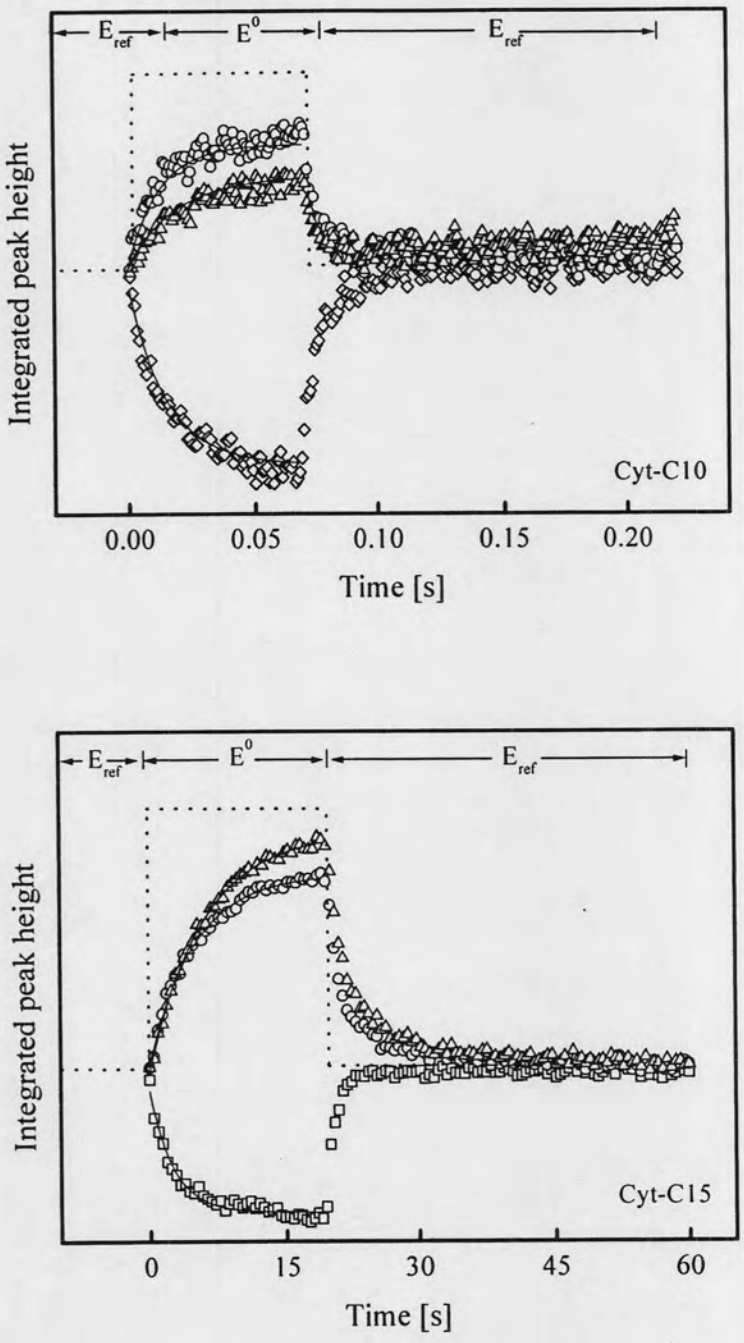

Figure 4.32 Kinetic traces of the time-evolution of the SEIRA bands at 1693 cm^{-1} squares; reduced), 1673 cm^{-1} (circles, oxidised), and 1660 cm^{-1} (triangles, oxidised) obtained from the rapid scan and step scan SEIRA spectroscopic measurements of Cyt-c on C10-SAM (top) and C15-SAM (bottom), respectively (see Figure 4.30 and 4.31).

Table 4.1 Relaxation constants for the potential jump from -0.1 V to the redox potential for Cyt-c immobilised on coated electrodes as determined by rapid scan and step scan SEIRA spectroscopy.[a,b]

system/technique			C15-SAM	C10-SAM	C5-SAM
SEIRA, Au[a]	1693 cm^{-1} (red.)	$k_{prot,relax}$	0.4 s^{-1}	75 s^{-1}	900 s^{-1}
		k_{prot}^{red}	0.2 s^{-1}	38 s^{-1}	450 s^{-1}
	1673 cm^{-1} (ox.)	$k_{prot,relax}$	0.2 s^{-1} (0.4 s^{-1})[b]	90 s^{-1}	700 s^{-1}
		k_{prot}^{ox}	0.1 s^{-1} (0.2 s^{-1})[b]	45 s^{-1}	350 s^{-1}
	1660 cm^{-1} (ox.)	$k_{prot,relax}$	0.2 s^{-1}	50 s^{-1}	600 s^{-1}
		k_{prot}^{ox}	0.1 s^{-1}	25 s^{-1}	300 s^{-1}
CV, Au		k_{redox}	0.2 s^{-1}	40 s^{-1}	240 s^{-1}[d]
		k_{ET}	0.2 s^{-1}	40 s^{-1}	
SERR, Ag[c]	heme modes	$k_{redox,heme}$	0.15 s^{-1}	85 s^{-1}	270 s^{-1}
		k_{ET}	0.08 s^{-1}	43 s^{-1}	
	heme modes	k_{rot}	> 6000 s^{-1}	350 s^{-1}	250 s^{-1}

[a] Kinetic data refer to pH 7.0 at at ionic strength of 66 mM. The rate constants are defined by eq (4.1). [b]Relaxation constant determined for an ionic strength of 22 mM (pH 7.0). [c]Taken from ref. 60 and 88. [d]Apparent rate constant reflecting a process other than electron tunneling.

Previous studies on Cyt-c immobilised on SAM-coated electrodes have revealed an unusual distance dependence of the electron transfer kinetics [34,60,89,90]. Whereas at SAMs with chain lengths longer than C10, the kinetics can be ascribed to an electron tunnelling mechanism, SAMs with shorter SAM lengths (< C10) show distance-independent rate constants implying that a process other than electron tunnelling is rate-limiting [3,4,34,60,91-93]. This phenomenon has been observed by various techniques and different electrochemical systems and proteins. In a recent SERR spectroscopic study, it has shown that this rate-limiting step is the re-orientation of the entire immobilised Cyt-c [88]. Since the orientation of the heme with respect to the SAM surface is a crucial parameter controlling the electron tunnelling rate, the rate of the overall redox process is modulated by the rate of re-orientation, which may be imagined as a rotational diffusion. This process, however, sensitively depends on the local electric field and thus its rate constant decreases from long to short SAM lengths, whereas for a given orientation the electron tunnelling rate increases exponentially with decreasing distance to the electrode.

For C15-SAM, the reorientation rate constant (k_{rot}) has been found to be larger than 6000 s^{-1} whereas for the redox transition a relaxation constant k_{redox} of 0.15 s^{-1} has been determined [60,88]. Since these SERR experiments like the present SEIRA measurements were carried out with potential jumps to the redox potential, the forward and backward electron transfer reaction ($k_{ET}^{ox}, k_{ET}^{red}$) are both associated with a driving force of 0 eV, i.e.

$$k_{redox} = k_{ET}^{ox} + k_{ET}^{red} = 2 \cdot k_{ET} \qquad (4.1)$$

such that the formal heterogeneous electron transfer rate constant k_{ET} is ca. 0.08 s^{-1}.

Unlike to SERR measurements that directly probe the redox state change of the heme, the kinetic constants derived from the SEIRA experiments refer to the temporal evolution of band intensities of the protein matrix (k_{prot}^{ox}, k_{prot}^{red}). These amide I band changes reflect structural and orientational changes of individual peptide segments that are induced by the redox state change of the heme and may occur with the same rate as electron tunneling, or may follow the electron transfer step. Thus, in the simplest case, one may describe the processes of Cyt-c that are induced by the

potential jump to the redox potential by the scheme sketched in Figure 4.33. For the potential jump from -0.1 V to the redox potential, SEIRA experiments monitor the oxidation of the immobilised Cyt-c (bold arrows in Figure 4.33).

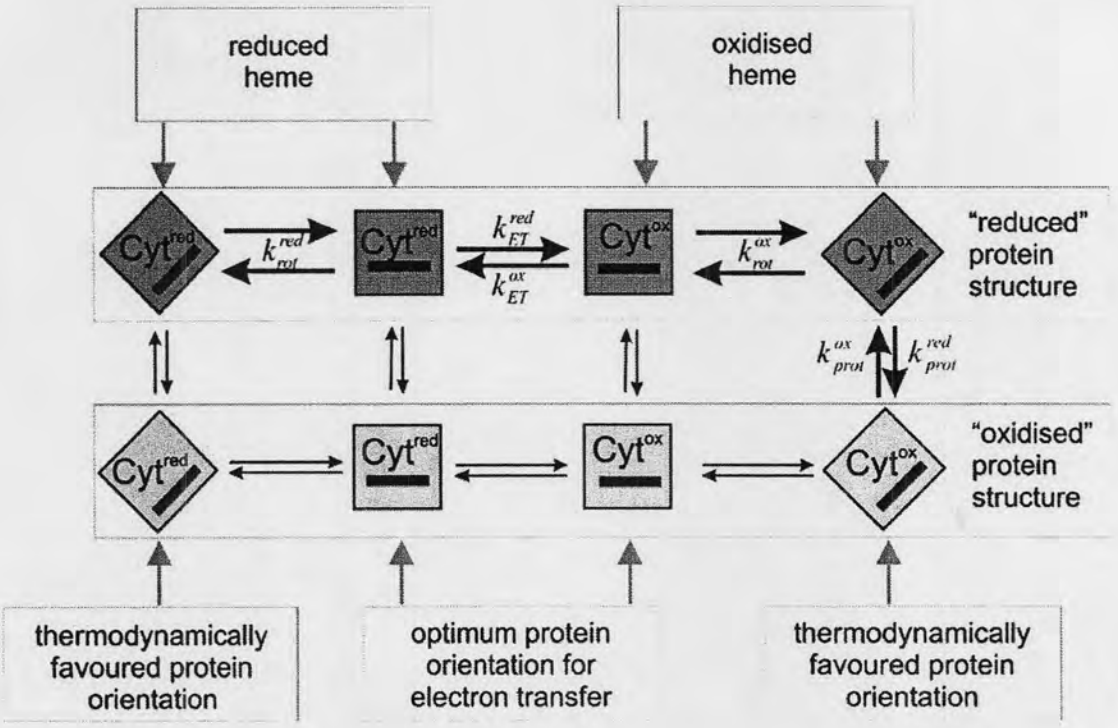

Figure 4.33 Model for the reaction mechanism of the interfacial redox process of Cyt-c immobilised on SAM-coated electrodes. The reaction pathway studied in this work is highlighted by the bold arrows. k_{rot}^{ox} and k_{rot}^{red} refer to the relaxation constants for rotational diffusion, monitored by TR SERR spectroscopy, whereas k_{prot}^{ox} and k_{prot}^{red}, derived from SEIRA measurements, denote the rate constants of the protein structural changes to adapt the equilibrium structure of the reduced and oxidised Cyt-c, respectively. k_{ET}^{ox} and k_{ET}^{red} are the standard heterogeneous electron transfer rate constants at zero driving force (see eq (4.1)).

4.6 Cyclic Votammetry

CV measurements were carried out with the SEIRA electrode. The area of the SEIRA active surface was determined according to

$$A_{real} = A_{geom} \cdot R_f \tag{4.2}$$

where A_{real} and A_{geom} are the real surface area and geometric area of the Au-electrode, respectively; Rf is the surface roughness factor,as defined in eq (4.3), obtained from the ratio between an experimental ($Q_{\exp}$) and theoretical (Q_{the}) charges, as well as the geometrical area of the electrode (A_{geom}), where the Q_{the} we used was 448 $\mu C \cdot cm^{-2}$ [94].

$$R_f = \frac{Q_{\exp}}{Q_{the} A_{geom}} \tag{4.3}$$

Accordingly, the $Q_{\exp}$ is obtained by integrating the cathodic peak for a reduction of the Au-oxide layer, which is assumed to be proportional to the actual area of the Au-electrode after electrochemically cleaned in sulfuric acid. Our $Q_{\exp}$ and A_{geom} have a value of 1100 $\mu C \cdot cm^{-2}$ and 0.9 cm^{-2}, respectively, thus the surface roughness factor of our SEIRA active Au-surface was calculated to be 2.8. The value is similar to that found by Miyake (R_f = 2.5) obtained with the same preparation for the SEIRA active surface [23]. Subsequently, the real surface area of 2.52 cm^2 of our Au-electrode could be determined.

Knowing the real area of the Au-electrode, the coverage of electrochemically active protein (Γ) was easily determined on the basis of CV scans according to

$$I_p = n^2 F^2 \upsilon A \Gamma / 4RT \tag{4.4}$$

where I_p, A and υ represent the average peak current, effective electrode surface and scan rate, respectively. According to the plot of relationship between I_p and υ,

an average surface coverage of the immobilized Cyt-c is estimated to be 8, 9 and 10 pmol·cm^{-2} for C15-, C10- and C5-SAMs, respectively. These values are somewhat lower than the theoretical maximum coverage of 15 pmol·cm^{-2} [81].

Figure 4.35 shows typical CVs for the immobilised Cyt-c on C5-, C10- and C15-SAMs coated electrodes. The CVs present clear redox peaks with small peak-to-peak separations (ΔE_p) for C10- and C5-SAMs. The voltammograms are nearly reversible with $\Delta E_p < 0.040$ V for CV scan rates up to 0.4 V/s and 1.5 V/s in the case for C10-SAM and C5-SAMs, respectively. Within these ranges of the scan rates, the full-width at half maximum is 0.09 - 0.12 V which is close to the reversible value of 0.1 V. Up to a scan rate of 8.0 V/s for C10-SAMs and 20 V/s for C5-SAMs, the peak separation is still less than 0.20 V. Because of the small electron transfer rate constant for C15-SAM, the voltammograms display deviations from the shape expected for a reversible behaviour since the peaks are broadened and ΔE_p is already larger than 0.2 V at a scan rate 0.05 V/s. The redox potentials of Cyt-c determined from cyclicvoltammograms were obtained from the anodic and cathodic peak potentials, E_{pa} and E_{pc}, respectively.

$$E^0 = \frac{E_{pa} + E_{pc}}{2} \tag{4.5}$$

The E^0 of the immobilised Cyt-c measured at an ionic strength of 66 mM (pH 7.0) is 0.036 V which is slightly negatively shifted from that of Cyt-c in solution (0.05 - 0.06 V).

As shown in Figure 4.35, the peak current increases linearly with the scan rate, indicating a surface-confined electrode process of the immobilised Cyt-c. Employing Laviron's method, the corresponding standard electron transfer rate constants k_{ET} can be deduced from the peak separation of the voltammogram vs the scan rate [95]. For $\Delta E_p < 0.2\,\mathrm{V}$, one obtains a value of 0.14, 40, and 250 s^{-1} for C15-, C10-, and C5-SAMs (Table 4.1), respectively.

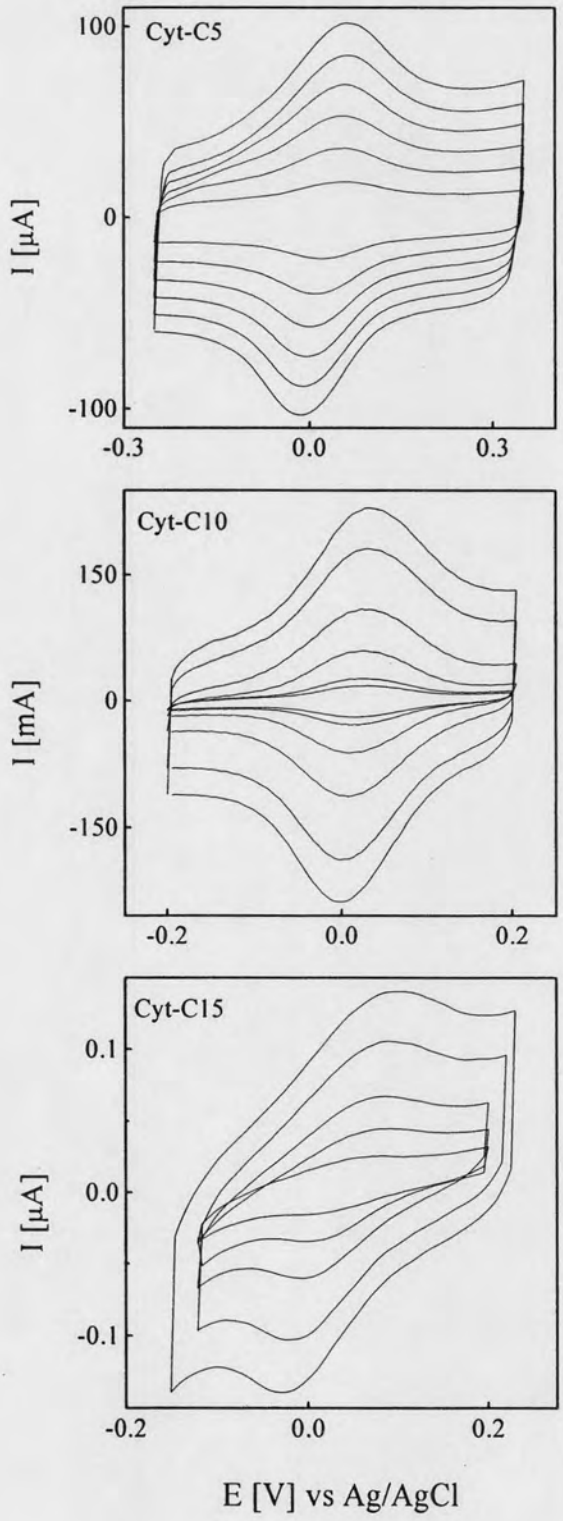

Figure 4.34 CVs of immobilised Cyt-c on C5-SAM (top) at scan rates of 1, 2, 3, 4, 5 and 6 Vs^{-1}, respectively; on C10-SAM (middle) at scan rates of 0.05, 0.10, 0.2, 0.4, 0.8 and 1.0 Vs^{-1}, respectively; and on C15-SAM (bottom) at scan rates of 1, 2, 4, 7.5 and 10 mVs^{-1}, respectively. The experiments were carried out at an ionic strength of 66 mM (pH 7.0).

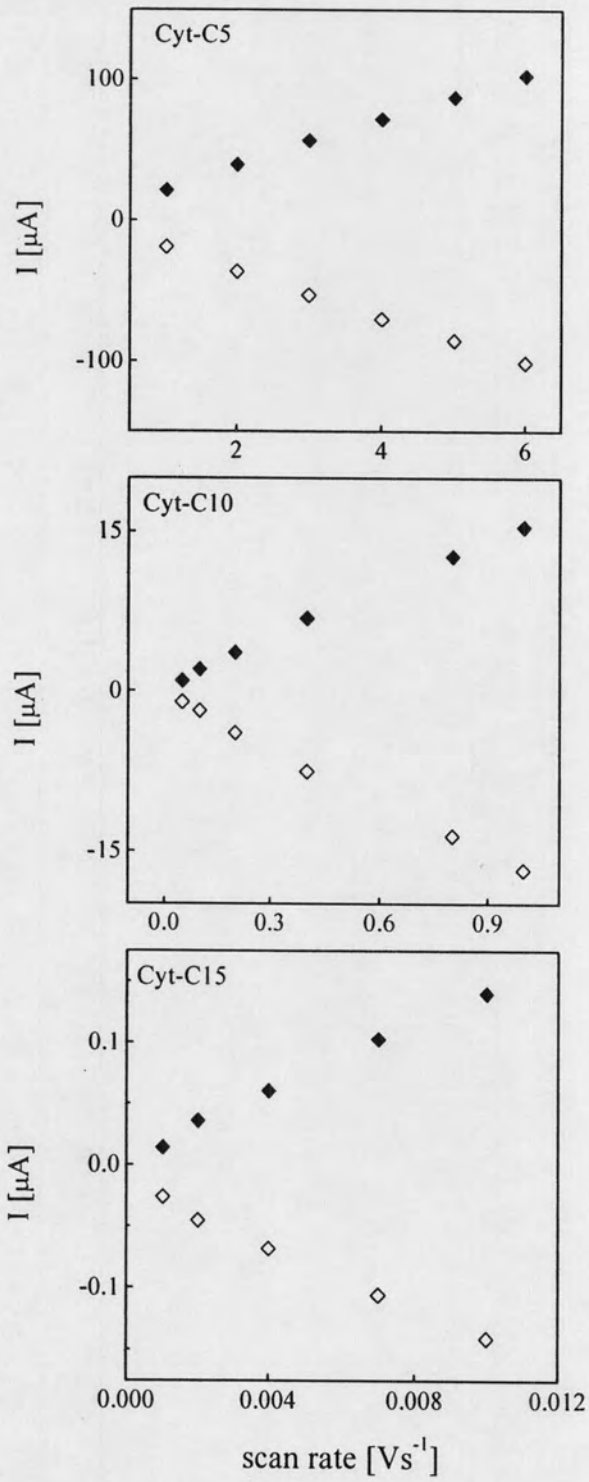

Figure 4.35 Relationship between peak current and scan rate derived from the CVs of immobilised Cyt-c on C5-SAM (top), on C10-SAM (middle) and on C15-SAM (bottom). Anodic and cathodic currents are given by close and open symbols, respectively. The experiments were carried out at an ionic strength of 66 mM (pH 7.0).

4.7 Electric Field Effects on the Interfacial Redox Process

Comparing the present results of the distance dependence of the ET dynamics with those previously obtained by TR SERR spectroscopy on Ag/SAM [60] and by electrochemistry on Au/SAM electrodes [89,90], consistent with the view that at SAM lengths shorter than C10 the overall rate of the ET process is limited by a reaction step other than electron tunneling and eventually becomes distance-independent. Differences are noted for the values of the rate constants for the rate-limiting step which for Au/C5-SAM (SEIRA, CV), is larger by ca. a factor of 2 than for Ag/C5-SAM (SERR) (Table 4.1). This discrepancy is attributed to the effect of the EF in the SAM/protein interface. For the Ag/SAM system this parameter has been shown to slow down the re-orientation of the immobilised protein (rotational diffusion) such that it becomes the rate limiting step at Ag/C5-SAM with $k_{rot} = 250\ s^{-1}$. We therefore assume that the EF is weaker in the SAM/protein interface on Au compared to Ag electrodes.

The EF strength at the protein/SAM interface can be described on the basis of a simple electrostatic model originally proposed by Smith and White [40] and later adapted to the electrode/SAM interface [26]. Accordingly, the electric field strength (E_{EF}) may be approximated by

$$E_{EF} = \frac{-\sigma_C . d_{RC} + \varepsilon_0 \varepsilon_P \left(E - E_{pzc}\right)}{\varepsilon_o (d_C \varepsilon_P + d_{RC} . \varepsilon_C)} \qquad (4.6)$$

Eq. (4.5) indicates that E_{EF} mainly depends on three parameters. It increases with decreasing distance to the electrode (d_C) and increasing charge density in the protein/SAM interface (σ_C). These two parameters may be similar albeit not identical for both the Au and the Ag electrode. The third parameter is the potential of zero charge E_{pzc} which is > 0.4 and ca. -0.7 V for Au and Ag, respectively [83-86]. Thus, for electrode potentials around the redox potential of Cyt, $E - E_{pzc}$ is negative for Ag but positive or close to zero for Au. Since σ_C is negative, the E_{EF} is larger for Ag than for Au. This conclusion is consistent with the fact that the potential-drop across the Au/SAM/Cyt interface which is reflected by a shift in the redox potential is much

smaller than for the Ag system. Correspondingly, one may readily rationalise the two-times slower kinetics of the rate-limiting step (i.e., protein rotation) on Ag/C5-SAM in terms the higher E_{EF} as compared to the Au/C5-SAM.

For longer chain lengths, electron tunneling is the rate-limiting step on both, the Ag/SAM and Au/SAM system. The values obtained for the ET rate constant obtained by CV (Au) and SERR (Ag) are the same for both metals for the C10-SAM, whereas for the C15-SAM somewhat larger rate constants are determined for the Au/C15-SAM system. This discrepancy may be due to a slightly different structural organisation of the SAMs on Au and Ag that may include different tilt angles of the aliphatic chains with respect to the surface [97-99]. This may have consequences for the tunneling distances for longer chain lengths (C15-SAM) and thus affect the ET rate constant. Note that just a decrease of the tunneling distance by 0.5 Å can readily account for the different rate constants determined for Au/C15-SAM and Ag/C15-SAM.

We cannot exclude that the ET affects the dynamics of the protein structural changes as monitored by SEIRA spectroscopy. However, the present data are consistent with the view that, regardless of the chain length and thus independent of the EF, the protein structural changes follow the electron transfer. Thus, the simplified reaction model depicted in Fig. 4.33 may represent a reasonable approximate description for the interfacial redox processes of Cyt-c in general.